

FINAL TECHNICAL REPORT

Project Title: Multiphase Nano-Composite Coatings for Achieving Energy Optimization

DOE Award Number: DE-EE0003489

Project Period: August 16, 2010 – December 31, 2011

Principal Investigator: Dr. Jose Nainaparampil
937 426 6900 X 209
jnain@ues.com

Recipient Organization: UES, Inc.
4401 Dayton-Xenia Rd.
Dayton, OH 45432

Partners: Argonne National Laboratory
Kapex Manufacturing
Triangle Precision Technologies

Date of Report: March 30 2012

ACKNOWLEDGEMENTS

This report describes the research, development and commercialization efforts of UES/Argonne National Laboratory (ANL) team on environmental and thermal-degradation resistant coatings developed for Department of Energy under the award # DE-EE0003489. The UES team players involved in this program are Dr. Josekutty Nainaparampil, Dr. Amarendra K. Rai, Dr. Rabi Bhattacharya, and Mr. Boris Brodkin. Dr. Ali Erdemir was the lead of the collaborative efforts of Argonne National Laboratory in this teamwork. The author thankfully acknowledges the valuable comments and guidance of Dr. Mahesh C. Jha, the Project Officer from DOE. The in-kind inputs in the form of services and tools of Mr. Paul Herzinger of Triangle Precision Industries and of Mr. James Kowalczyk of Kapex Manufacturing are thankfully acknowledged.

The author would also like to acknowledge the outstanding administrative support of Ms. Jan Clark throughout this Project.

NOTICE

This report was prepared as an account of work sponsored by the United States Government. Neither the United States Department of Energy , nor any of their employees, nor any of their awardees, subcontractors, or their employees, makes any warranty express or implied, or assumes any legal liability or responsibility for the accuracy, completeness, or usefulness of any information, apparatus, product or process disclosed or represents that its use would not infringe privately-owned rights.

TABLE OF CONTENTS

	Page
ACKNOWLEDGEMENTS	2
LIST OF ACRONYMS	4
LIST OF FIGURES	5
LIST OF TABLES	7
EXECUTIVE SUMMARY	8
1.0 INTRODUCTION	10
2.0 BACKGROUND	11
3.0 EXPERIMENTAL	13
3.1 DEPOSITION TECHNIQUE	13
3.2 CHARACTERIZATION	14
3.2.1 In House Machining Test Facility	14
3.3 ACCELERATED EVALUATION OF TOOL COATING PERFORMANCE BASED ON OPTICAL MICROSCOPY	16
3.3.1 Optical Microscopy of used Tools to Measure the Wear Related Degradation	17
3.3.2 Calculation of the Burned Out Volume	18
3.3.3 Optical Microscopy of Burned Tips Surface Measurements	19
3.4 IN HOUSE THERMAL CYCLING TEST FACILITY	20
4.0 RESULTS AND DISCUSSION	21
4.1 CUTTING TOOL COATINGS	21
4.1.1 In House Study	21
4.1.2 Industrial Level Study	23
4.1.3 Cutting Chips Study	29
4.2 DIE CASTING COATINGS	31
4.2.1 In House Study	31
4.2.2 Failure Analysis of Core Pins	31
4.2.3 Optical micrograph Surface Study	31
4.2.4 Local Coating Failure	33
4.2.5 Pit Formation	33
4.2.6 In-depth Growth of a Pit	38
4.2.7 Titan Generation II Coating and TitanCoat TM	38
4.2.8 Titan Generation II, Industrial Level Study	42
4.3 ARGONNE NATIONAL LABORATORY COATINGS	42
4.3.1 Deposition System	42
4.3.2 Results	43
5.0 BENEFITS ASSESSMENT	51
6.0 COMMERCIALIZATION	52
7.0 CONCLUSION	53
8.0 ACCOMPLISHMENTS	54
9.0 REFERENCES	55

LIST OF ACRONYMS

MQL	Minimum Quantity Lubrication
CVD	Chemical Vapor Deposition
CTE	Coefficient of Thermal Expansion
LAFAD	Large Area Filtered Arc Deposition
X- SEM	Cross sectional Scanning Electron Microscopy
EDS	Energy Dispersive Spectroscopy
RPM	Revolutions per Minute
PVD	Physical Vapor Deposition
SEM	Scanning Electron Microscopy

LIST OF FIGURES

	PAGE
FIGURES	
Figure 1. Schematic diagram of the Large Area Filtered Arc Deposition system (LAFAD)	14
Figure 2. Pro-Track CNC CMX mill used for in-house testing of tool coatings	15
Figure 3. Photographs showing the index-able end-mill carrying the inserts	15
Figure 4. Typical coated inserts used in the accelerated tool deterioration study.....	15
Figure 5. Schematic showing three main heat sources in cutting	16
Figure 6. Burned area of a typical used insert (uncoated).....	17
Figure 7. Relationship between length scales and the surface area to volume ratio for standard geometries.....	18
Figure 8. The graph connecting the surface to volume ratio for different size scale of a tetrahedron.....	18
Figure 9. The burned-out area discoloration and contrast change as detected for three sides of an uncoated tool.....	19
Figure 10. Schematic diagram showing the definition of length scale estimation.....	19
Figure 11. (a) Control board and mechanical arms (b) Molten Al bath (c) Cooling water reservoir	20
Figure 12. The burned-out area discoloration and contrast change as detected for three sides of each Triangular inserts used for coating evaluation	22
Figure 13. Total burned-out volume of various coatings compared to uncoated sample	23
Figure 14(a). Uncoated Carbide Cutting tool received from Triangle Precision that are used in steel machining (lower numbers designates the tool type).....	24
Figure 14(b). Carbide Cutting tool coated with Greycho II TM coatings provided to Triangle Precision for steel machining	24
Figure 15. Coating performance, UES vs. Commercial coatings (Triangle Data).....	25
Figure 16(a). Uncoated Carbide Cutting tool received from Kapex that are used in hard steel machining.....	26
Figure 16(b). Modified GreychoTM coated Carbide Cutting tool provided to Kapex that are used in hard steel machining	26
Figure 17(a). Digital micrographs of tools provided to Kapex after 12 hours of severe roughening	27
Figure 17(b). Digital micrographs of commercial tools after 4 hours of severe roughening.....	27
Figure 18(a). Digital micrographs of flutes showing cutting edges coated with Greycho II™	28
Figure 18(b). Digital micrographs of flutes showing cutting edges coated with Commercial coating.....	28
Figure 19. Performance of UES coated Kapex tools compared to commercial coatings	29
Figure 20. (a) Optical micrograph showing chips (4 hours) collected from commercially coated tools and (b) Optical micrograph showing chips collected (12 hours) from UES coated tools	30
Figure 21. (a) Optical micrograph showing single chip (one hour) collected from commercially coated tools and (b) Optical micrograph showing chips collected from UES coated tools (ten hours)	30
Figure 22. Optical micrograph (50X) of the thermally cycled surface coated with (A) Uncoated pin,.....	32
Figure 23(a). Cross section of uncoated pin showing numerous pits formed into the H-13 substrate.....	34
Figure 23(b). Cross section of uncoated pin showing the detailed structure of pits	34
Figure 23(c). Cross-section of Titan Generation I coated pin showing failure of the coating and pits	35
Figure 23(d). Magnified cross-section of Titan Generation I coated pin showing delamination of the coating and steel surface degradation.....	35
Figure 23(e). Cross-section of modified Titan Generation I coated pin showing overall performance.....	36
Figure 23(f). Magnified cross-section of Titan Generation I coated pin showing delamination of the coating and steel surface degradation.....	36

LIST OF FIGURES (CONT.)

FIGURES	PAGE
Figure 23(g). Cross section of Titan Generation II coated pin showing undisturbed coating and steel surface	37
Figure 23(h). Magnified cross section of Titan Generation II coated pin showing undisturbed coating and steel surface	37
Figure 24. EDS data inside a pit showing the major elements (uncoated pin)	38
Figure 25. Metal dissolution/thermal stress dipping test results.	40
Figure 26(a). SEM micrograph showing X-section of bare rod.....	41
Figure 26(b). SEM micrograph showing X-section of Titan coated rod	41
Figure 26(c). SEM micrograph showing X-section of Titan Generation II coated rod	41
Figure 27. End mills and triangular cutters coated with MoN-Cu using the sputter ion plating process.....	43
Figure 28. Rockwell C (a) middle, (b) 1st corner and (c) 2nd corner on steel witness.....	43
Figure 29(a). Friction trace, Friction coefficient Vs Time.....	44
Figure 29(b). Wear scar of MoN-Cu flat	44
Figure 29(c). Wear scar profilometry of the flat with line scan	44
Figure 29(d). 3D-Wear scar profilometry of the ball.....	45
Figure 29(e). Ball micrograph.....	45
Figure 30(a). Friction trace, Friction coefficient Vs Time.....	46
Figure 30(b). Wear scar of MoN-Cu flat	46
Figure 30(c). Wear scar profilometry of the flat with line scan	46
Figure 30(d). 3D-Wear scar profilometry of the ball	47
Figure 30(e). Ball micrograph.....	47
Figure 31(a). Friction trace, Friction coefficient Vs Time.....	48
Figure 31(b). Wear scar of MoN-Cu flat	48
Figure 31(c). Wear scar profilometry of the flat with line scan	48
Figure 31(d). 3D-Wear scar profilometry of the ball	49
Figure 31(e). Ball micrograph.....	49
Figure 32(a). Friction trace, Friction coefficient Vs Time.....	50
Figure 32(b). Ball micrograph (reasonable wear).....	50

LIST OF TABLES

TABLES	PAGE
Table 1. Machining Conditions.....	17
Table 2. Cutting Parameters.....	25
Table 3. Wear area of tools coated with UES and commercial coatings	29
Table 4. Record of Production Cycles using the Titan Generation II Coated Pins.....	42

EXECUTIVE SUMMARY

Two industrial areas of elevated energy consumption are the aluminum die-casting and the machining used for the formation of various engine parts. Thermal degradation of die components and tools cause significant issues for the die-casting industry and machining because of their high manufacturing and replacement costs. Wear, a thermal degradation mode of the involved materials is caused primarily due to the necessity for multiple reuses for a typical production run. The purpose of this project was to conduct cost-shared research, development, and commercialization of innovative mechanical, environmental and thermal-degradation resistant coatings utilizing novel processes to make industrial components last longer and operate in harsher and higher temperature environments. These advances were accomplished to a reasonable level as demonstrated at laboratory level and in some of the industrial level applications.

UES/ANL team investigated in detail and identified the relevant issues that need to be addressed in machining and die casting tool degradation problems. Appropriate coatings with required characteristics to address effectively these problems were identified as a solution to this. After developing these coatings, the specific goals of the project were achieved by following effective process of in-house testing followed by the industrial partner testing of the potent high performing coatings. Appropriate techniques for in-house evaluations were designed and applied successfully to optimize effective coating technologies and its applications.

One of the significant accomplishments achieved in this project is a novel cutting tool coating (GreychoTM) that is conformal with complex contour of the cutting tools and brought significant improvement to tool life (almost 6 times!) as reported by our industrial partners after their commercial use. The other significant accomplishment achieved in this project is a novel die casting coating, Titan Generation II TM, which is temperature resistant, well-adhered dense film, which brought significant improvement to die casting tool as reported by Honda Manufacturing from their commercial use. These coatings matched or exceeded their goals set for the standard cycle goal for V6 model and the goal for R40 model, which are 15000 shots higher than the old standard goal.

These material systems are developed for applications in fabricated metal product section of manufacturing that consumed 388 trillion Btu in 2008. To estimate the machining sectors' energy saving potential, it was assumed that new coatings developed in this project would gain one-third of the market share by 2022 and these coatings are at least able to improve tool life by a modest 2X (over current average tool life). The U.S. annual energy saving would be close to 71.5 trillion Btu/year. With further optimization, we expect 5 to 6X improvement in tool life; hence, energy saving figures will be much higher. Furthermore, with widespread utilization of high speed machining, the productivity will increase plus fewer machine down time and reject parts resulting from the uses of new coatings are expected to result in additional savings.

The coatings developed in die casting area can save energy in the metal casting industry that uses an estimated 200 to 250 trillion Btu per year. This includes energy from electricity, natural gas, propane and fuel oil. The energy used in metal casting is mostly in the melting, molding and heat treatment process. Metal casting industry sales in the United States have been in the range of \$25 to \$28 billion annually for the past several years, with a small trade surplus. There are close to 3,000 foundries operating in all 50 states, employing one-quarter of a million people. The die-casting industry estimates show that 25% of the cost of the products (valued at nearly \$ 6.25 to 7 billion; (www.afsinc.org) is accounted for by the energy consumption. Thus, longer die life and longer production cycles will make a significant impact on the overall energy consumption rate (in terms of BTU/ton of product shipped), if

developed coatings can be successfully implemented and commercialized. A 5% savings in energy would lower the energy consumption by 10 to 12.5 trillion Btu.

As a commercialization effort for these novel high performing coatings, UES plans to approach our present customers. UES is a Tier1 supplier to Honda of America for coated core pins. In addition to our technical expertise, we recently established a Business Development group comprised of a senior manager, a direct sales engineer, and marketing and commercialization specialists. These personnel are assisted in the commercialization process by UES management and the Board of Directors. We have the appropriate technical and business teams in place to engineer the proposed technology, and bring it to market.

1.0 **INTRODUCTION**

The machining industry is constantly seeking ways to enhance performance (metal removal rate), durability, and productivity (reduce cost) of the manufactured parts. One way to enhance machining performance is to utilize high speed machining. One of the problems associated with high speed machining is increased wear, leading to reduction in tool life. This is essentially due to higher cutting temperature generated between the tool tip and the component interface. Higher cutting temperature can also increase the chemical reactivity between tool and work piece materials. This can lead to increased chemical wear, further reducing tool life. Shorter tool life leads to frequent tool changes and increased machine down time. This, in turn, reduces overall productivity. Hence, it is desirable to minimize the cutting temperature and/or the chemical reactivity.

Conventionally the cutting temperature is lowered by the use of metal-cutting fluids (coolants). However, due to safety and environmental concerns, the use of coolant is not desirable. Coolant less or minimum quantity lubrication (MQL) machining can also minimize cost and energy consumption.

In conventional machining, generic coatings such as TiN, TiAlN, CrN, and CrAlN are being used to impart wear resistance to the cutting edges of the machine tool (longer tool life). These coatings do not provide sufficient protection of the tools in high-speed, dry or MQL machining because the temperature generated in these types of machining is very high resulting in very high wear of tools. To mitigate issues associated with high-speed machining, multifunctional coatings having higher temperature stability, higher wear resistance and lower friction than the currently used coatings are needed.

Another area of high-energy consumption is the aluminum die-casting used extensively in the automotive industry. Thermal degradation of die components is a significant issue for the die-casting industry because of their high manufacturing and replacement costs. Wear, a thermal degradation mode of the die is caused primarily due to the necessity for multiple reuses of the die for a typical production run of more than 100,000 castings at the rate of 2500 shots per day. For this rate of production, it is required that the molten metal be introduced into the die cavity at high flow velocities (typically 40m/sec) and rapidly solidify for quick forming and ejection. This quick thermal cycling results in die temperature gradients about 1000°C/cm. Thus, the dies are subjected to very harsh conditions combining high temperatures, molten metal impingement, high injection pressure, and thermal cycling. These extreme and rapid cycling conditions take their toll on components of the die assembly such as the ejector and core pins. Consequently, the die-casting industry is subject to significant expenses in terms of die /component failures and their disposal, loss of productivity, and product quality problems. Thus, developments of approaches that can improve the life of dies/components are of paramount importance in terms of cost and energy savings, and improvements in industrial productivity.

The overarching goal of this project was to conduct cost-shared research, development, and commercialization of innovative mechanical, environmental and thermal-degradation resistant coatings utilizing novel processes to make industrial components last longer and operate in harsher and higher temperature environments.

2.0 BACKGROUND

The most often used coatings for machine tool protection are TiN, CrN followed by Ti(N,C), TiAlN and CrAlN [1,3]. In addition to these, for some applications ZrN, Cr(C,N) and (Ti,Zr)N are also applied [4-6]. The coatings can be deposited with different architectures like monolithic, multiphase, bilayered and multilayered. Depending on the ratio of layer thickness (t) to grain size (D) these coatings can be divided into three categories. (i) $t/D \gg 1$ (ii) $t/D = 1$ and (iii) $t/D < 1$. By varying the t/D ratio within the coating, the number of interfaces will be altered and hence mechanical properties like crack propagation and the hardness. All these architectures are applicable to different machining conditions [7-9]. At UES a TiAlN based bi-layered coating has been developed to enhance the cutting tool life in titanium machining application [10]. Hard-soft coatings have also been developed at UES and evaluated for enhanced tool life in various machining applications [11]. Compositionally gradient coatings are also applied in cutting tool application. In these coatings, a continuous change in the concentration of Ti, N, Cr and Al is used to design continuously changing mechanical as well as chemical reactivity property [12].

Most of the present day coatings are deposited with either physical vapor deposition (PVD), or with high temperature chemical vapor deposition (CVD) techniques. For adequate performance of the coating in machining application the coating should be dense and highly adherent to the substrate. Such qualities of a coating in a physical vapor deposition (PVD) technique can be obtained by high ionization efficiency of the process. Among the known PVD techniques, cathodic arc evaporation produces the highest degree of metal ionization. In the conventional (direct) cathodic arc process metal macroparticles are created due to localized arc melting of the metal target. The macroparticles are generally electrically neutral and therefore they do not combine with reactive gas and remain as metal particles in the hard (nitride, carbide) phase. Macroparticles in the coating can be avoided by a filtered arc deposition technique that in turn can provide a very smooth and highly dense and adherent coating. As described in section 3.1, filtered arc sources can also be utilized for efficient cleaning of the cutting tool surface which in turn could provide enhanced coating adhesion. Standard CVD process is done at temperatures higher than 800°C. Most of the tool steels become soft or compositionally compromised at these elevated temperatures. Besides coating adhesion, another limiting factor for the commonly used coatings is the lack of high temperature oxidation resistance inherent with their material systems [13]. Even though TiAlN could overcome this to a certain extent, lack of toughness of this material poses problems.

In the current project, UES has addressed the aforementioned issues by developing a more reliable material system suitable for high temperature operations usually encountered in high speed machining and by utilizing a large area filtered arc deposition (LAFAD) system (described in section 3.1).

This material system is developed based on a low temperature CVD process that guarantees tool steel property preservations and conformal coverage on complicated tool geometries. A multiphase multi-layer architecture is envisaged to bring out all the good qualities of this technology.

The three main failure mechanisms leading to die degradation in die-casting industry are corrosion/soldering, erosive wear and thermal fatigue. The issues of corrosion/soldering and erosion in die-casting industry, have been remedied sufficiently by surface engineering including nitriding/carburizing, hard coatings and duplex treatments [14]. They have reduced die erosion/wear from the impingement of the molten aluminum and suppressed the corrosion/soldering. However, the improvement in the thermal fatigue resistance is still limited. It has been found that the thermal fatigue cracking (heat checking) in the surface engineered coating is generated by the residual stress release due to coefficient of thermal expansion (CTE) mismatch. Cracks in the coating form brittle Fe-Al-Si ternary

intermetallics that fractures leaving a defect in the die surface. The conjoint action between the thermal fatigue cracking and chemical attack intensifies the degradation.

In the past, UES has developed TitanCoat™ for dissolution prevention in core pin aluminum (Al)-die casting. TitanCoat, which showed promising results, is based on filtered cathodic arc TiN based multilayered coating architecture [15]. UES is a Tier one supplier of TitanCoat™ to Honda of America. Even though this coating could easily attain the initial goal set for the life of core pins, the new goal set by Honda was unattainable with this coating. In the current project, UES has developed a novel low temperature CVD process to match or exceed the new goal of Honda for the life of core pins by utilizing a new material system based on HfB₂. Low temperature CVD process was conducted in the LAFAD system.

In this program, the processing conditions were optimized through evaluation of the relevant coating characteristics such as microstructure, thickness, hardness, wear, friction, adhesion, stress and toughness. The performance of the developed coatings was evaluated at in-house laboratory tests and at industrial partners. In this project, our industrial partners were Triangle Precision Technologies and Kapex Manufacturing who supplied us cutting tools and Honda of America who supplied Al-die casting pins. Further optimization of the coatings was based on demonstration tests. Failure modes of the coated tools and other relevant surfaces were analyzed.

3.0 EXPERIMENTAL

In this section, coating deposition techniques and characterization methods are described. An accelerated tool testing method is developed and described here that could reasonably predict the outcome of commercial application of our coated tools. Also in this section, we describe our CNC machining facility and thermal cycling facility.

3.1 DEPOSITION TECHNIQUE

A large area filtered arc deposition (LAFAD) system available at UES was used to deposit the proposed composite coatings. The substrates were supplied with a dynamic DC bias that can enhance adhesion and increase density of coatings. The technique uses low processing temperatures using energetic plasma enhanced beams in conjunction with conventional deposition techniques. The plasma generated by the arc has a large concentration of metal ions and the positive ion current is a constant fraction of the arc current that varies between 6-12 % of the arc current [16]. Apart from the multiplicity of charge states in the emitted ions, the intrinsic ion energy is considerably higher in comparison to that of evaporated or sputtered atoms. Ion energy measurements have shown energies of the order of 25 eV for C and 45 eV for Ti [16]. In addition to the generation of energetic plasma, the arc discharge also produces small liquid droplets commonly referred to as macro particles. The macro particle size ranges from 0.2 to 100 μm although some recent evidence suggests that smaller numbers of nano-particles (<100 nm) are also generated [16]. For this reason considerable efforts have been made in recent years to reduce or eliminate droplets using various forms of macro particle filters.

A schematic diagram of the coating deposition system is shown in Figure 1. Essentially the system consists of a rectangular chamber with two large area filtered arc sources and deflecting magnetic coil assembly, and a cylindrical deposition chamber with two direct arc sources and an auxiliary anode assembly. The direct arc sources can be replaced by two magnetron sputter sources thus enabling a hybrid coating deposition process combining filtered arc and sputtering. Appropriate gases were introduced into the deposition chamber for reactive deposition. The auxiliary anode assembly facilitates the generation of a highly ionized metal and/or gas plasma in which the substrate can be immersed. The deposition chamber has a built-in carousel type double planetary rotation system for mounting substrates. Overall, the system is capable of accommodating relatively large complex shaped parts for coating deposition.

The filtered arc sources were operated in two different modes viz., with magnetic field on or off. In the magnetic field on situation, the arc metal plasma is deflected along the curvilinear path towards the substrate. In this process, the macro particles having straight trajectories are filtered out and are captured on the baffles. Thus, only ionized metal plasma enters into the deposition chamber and deposit on the substrate. For harder nitride/carbide coatings appropriate gases viz. nitrogen/carbon based gases can be bled into the chamber to combine with the appropriate metal plasmas. Scanning of the filtered arc metal plasma in combination with the double planetary substrate rotation, allowed uniform coating deposition on the substrates with complex geometry.

In the magnetic field off mode, only the electrons (and not the metal ions) can be extracted from the filtered arc plasma into the deposition chamber to obtain highly ionized glow discharge plasma of a proper gas. This mode of operation is suitable for controlled surface cleaning of cutting tools/core pins (substrates) by appropriately biasing the substrates. Appropriate surface cleaning is essential for enhanced coating adhesion.

The magnetic field off mode can also be utilized for low temperature CVD process. For low temperature CVD process, a precursor gas for a given coating material can be introduced in the chamber

having highly ionized glow discharge plasma. The organic content of the precursor gas is expected to be removed in the highly ionized plasma (without high temperature) and eventual deposition of the inorganic (condensable) part on the substrate.

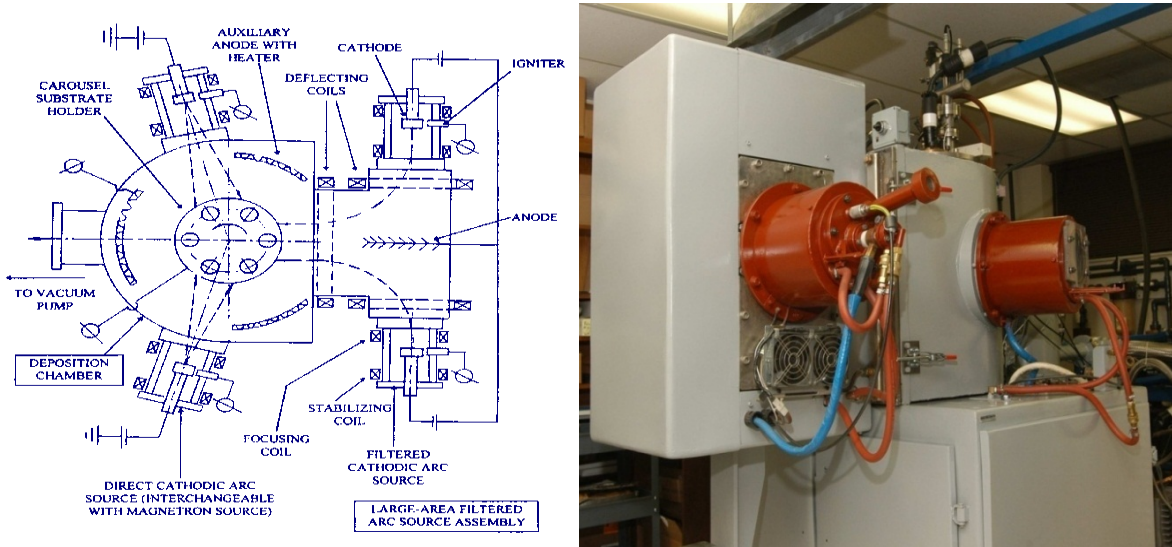


Figure 1. Schematic diagram of the Large Area Filtered Arc Deposition system (LAFAD)

3.2 CHARACTERIZATION

Deposited coatings were characterized for the microstructure, chemical composition, mechanical properties, erosion, and temperature stability. Cross sectional scanning electron microscopy (X-SEM) was used to characterize the microstructure, energy dispersive spectrometry (EDS) was used to analyze the chemical composition. Hardness was studied by nano-micro indentation. Mercedes indentation and diamond stylus scratching were used to study adhesion and ball on plate wear and friction test was used to study the durability. Thermal stability was studied by the thermal cycling of these samples between room temperature and 800°C in atmospheric conditions as well as in molten Al.

Following are the three major coatings developed in this project for tool applications and die-casting:

- 1) Greycho-I™ (TiN based)
- 2) Greycho-II™ (CrAlN based)
- 3) Titan Generation II™ (HfB₂ based)

3.2.1 In House Machining Test Facility

An index-able end-mill with two triangular inserts was used as milling edges. These inserts were used in dry cutting condition on a Pro-Track SMX CNC mill (see Figure 2). It is a programmable cutting mill that kept the parameters constant for each pass in each test. Figure 3 shows the index-able end mill carrying the triangular inserts. The diameter of the cut from edge to edge is 31.75 mm. At 1200 RPM, this gives a cutting speed of 120m/min. Obviously, it is in high-speed cutting regime.

Figure 4 shows the typical triangular insert used in this study. The actual volume of burned out tool is too small to measure. However, from the relationship between the surface area and the volume of small dimensional geometries, the burned out volume can be easily calculated. Optical microscopy with digital recording was used in this method. The next section describes this method in detail.



Figure 2. Pro-Track CNC CMX mill used for in-house testing of tool coatings



Side view



Top view

Figure 3. Photographs showing the index-able end-mill carrying the inserts

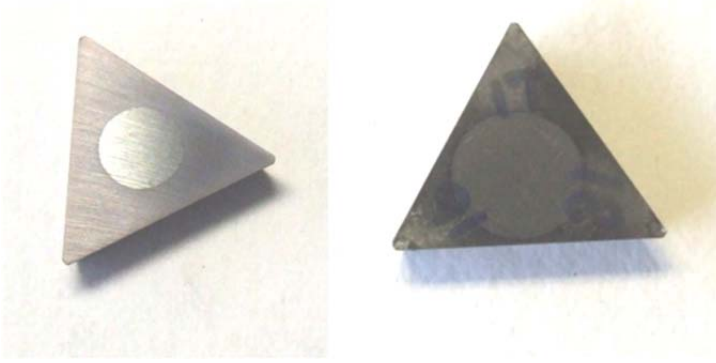


Figure 4. Typical coated inserts used in the accelerated tool deterioration study

3.3 ACCELERATED EVALUATION OF TOOL COATING PERFORMANCE BASED ON OPTICAL MICROSCOPY

The heat flux introduced into the cutting tool comes from the following three sources (Figure 5) heat from the primary shear zone (plastic deformation and viscous dissipation), heat from the secondary shear zone (frictional and plastic shearing energy), heat from the frictional rubbing of the work piece on the tool insert flank (tertiary shear zone). These heat sources diffuse either in the work piece, in the substrate or in the chip body. In fact, the quantification of these three sources remains unclear in both cases of uncoated or coated cutting tools. Moreover, the influence of a coating on the level of heat created by these heat sources is unknown.

Therefore, it is not obvious whether coatings influence the cutting process by an insulation effect (lower heat transmitted into the substrate), and/or by a tribological effect (lower level of heat created in the sources). Whatever it is, the heat generated in cutting process is the primary cause for the tool degradation. The volume of the tool burned-out in this heat is the basic factor affecting the tool life. Discoloration on the tool surface and the extent of discoloration acts as a significant signal before a catastrophic failure of the tool occurs. The obvious reason for this discoloration is the temperature gradient that is occurring during the cutting process. By observing this discoloration by an optical microscope the color change area can easily be detected and measured. Tools with maximum-burned volume (spread of discoloration) eventually cause the tool to chip and break away in catastrophic failure. This observation paved the basis for the accelerated evaluation method developed here. Figure 6 shows the typical burned-out pattern observed on tool edges (insert edge). The actual volume of burned out tool is too small to measure. However, the relationship between the surface area and the volume of small dimensional geometries could help to assess the burned-out volume.

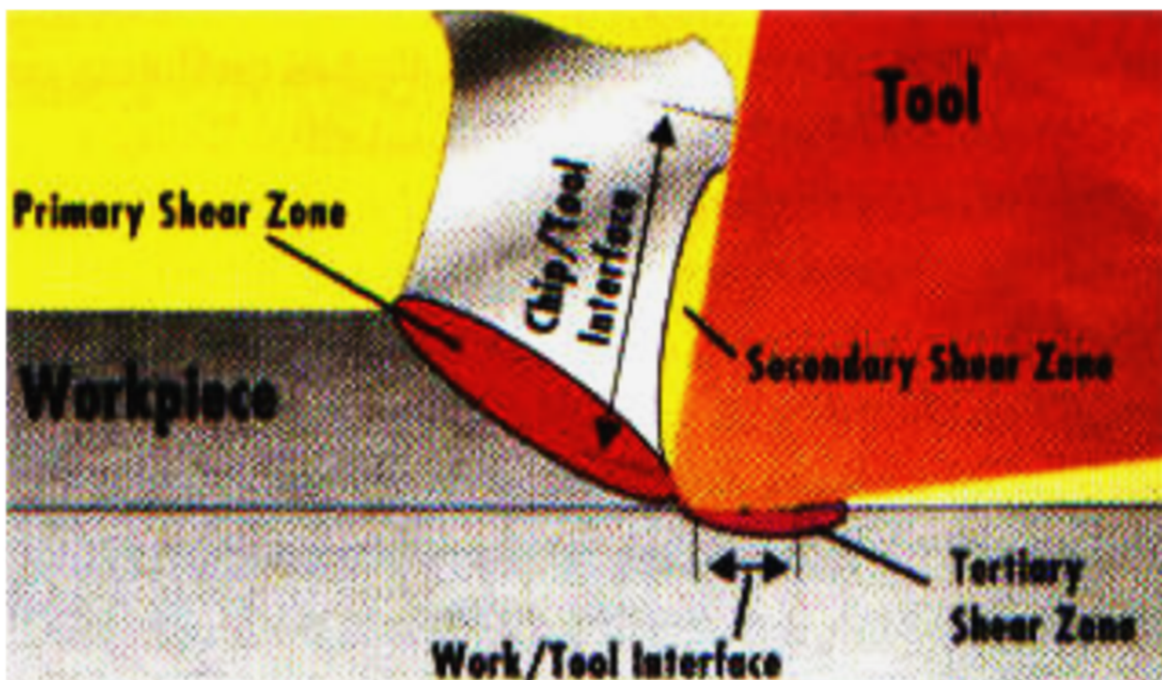


Figure 5. Schematic showing three main heat sources in cutting

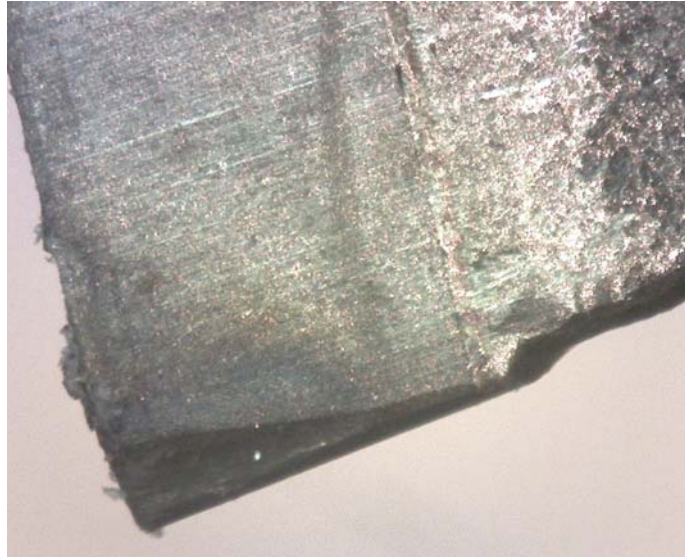


Figure 6. Burned area of a typical used insert (uncoated)

3.3.1 Optical Microscopy of used Tools to Measure the Wear Related Degradation

In this work, we have used an insert with three sides joining at a vertex of making approximately 60-90-90 degree angles between each edge (rectangular prism geometry, See Figure 6). Since the rake face is triangular and the insert can be mounted in three different positions, we can get three trials out of a single insert. We coated three of such tools with Greycho-I and Greycho-II. These tools were used to cut 12-20 rolled iron work-piece. The cutting conditions are given in Table 1.

Table 1. Machining Conditions

Spindle Speed (RPM)	1200
Diameter	31.75 mm
Cutting Depth	.015 inches
Travel	10 in/min
Work Piece	10-20 rolled steel
Tool Material	Carbide

All of these three tools were used in similar condition with same cutting parameters. These used tools were observed for deterioration under an optical microscope. Pictures were captured in jpeg format with *same pixel density* for each picture. The burned out-worn area detected from the wear related discoloration- and contrast changes are noted. After recording the pictures of each side of the tool, actual burned out area was measured using special software called Image J developed by NIH for image processing [17]. Adding three burned-out areas for each tool tip, the total burned out surface area S was calculated for each tip. The total burned out volume is calculated from the total burned out surface area using a conversion index determined from the property of geometrical shapes as described below. Figure 7 shows graphs connecting length scales and ratio of surface area to volume of standard geometries. Our cutter tip geometry is considered to be a tetrahedron.

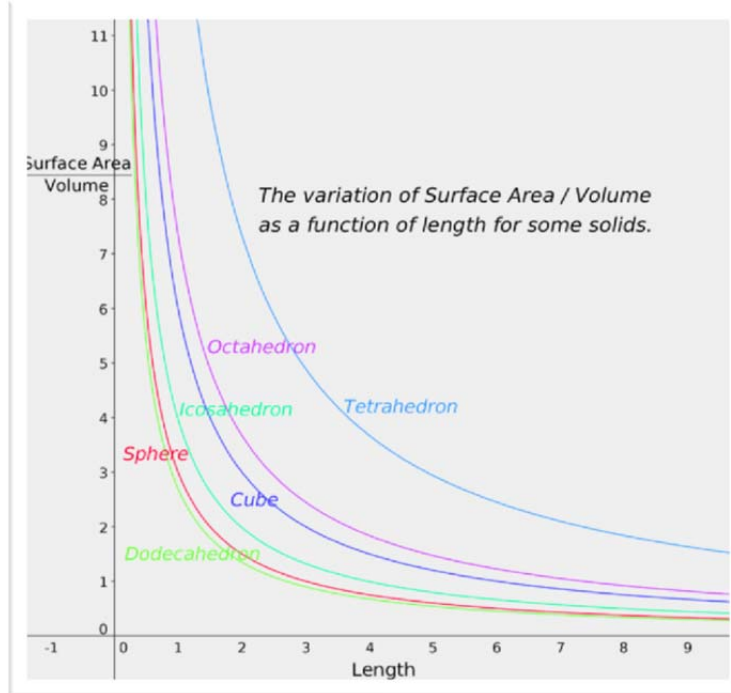


Figure 7. Relationship between length scales and the surface area to volume ratio for standard geometries

3.3.2 Calculation of the Burned Out Volume

Calculation of the burned out volume is based on the function connecting the size and the surface area to volume ratio of standard geometrical shapes described in the previous section. Figure 8 gives the graph connecting the surface to volume ratio and size scale of a tetrahedron. From this assumption, we can estimate the volume of the affected tool region from the graph shown in Figure 8 as follows.

It can be seen that for any geometrical shape as the size get smaller the surface area to volume ratio get bigger (Figure 7). That means the small-burned volume in the used tool tips can be easily assessed by measuring the surface area measurements of the same geometrical shapes and thereby we can compare the efficiency of the coatings in protecting the tool tips from the so-called burned-outs.

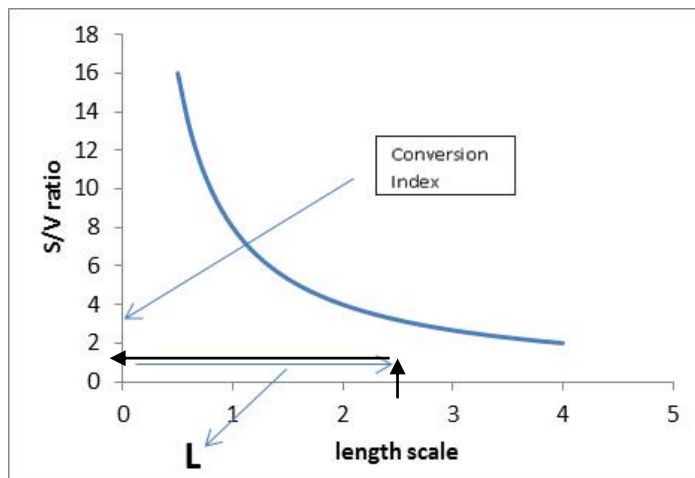


Figure 8. The graph connecting the surface to volume ratio for different size scale of a tetrahedron

3.3.3 Optical Microscopy of Burned Tips Surface Measurements

In this section, burned our surface area measurement is described using an uncoated rectangular tool tip. The used tool is examined under an optical microscope and pictures were captured in jpeg format with same pixel density for each picture. The burned out area detected from the discoloration and contrast change was marked by a pattern as shown in Figure 9. As described before, for each side of the tool, actual burned out area was measured with the help of special software referred before. Adding three burned-out areas for each side, total burned out surface area was calculated. The minimum burned-out area shows the least damaged volume of the tool. The tool with minimum burned-out volume indicates maximum tool life.

The burned out volume of each used tool can be calculated as follows. Let the length scale L of the affected region of tool be calculated from the edge lengths L_1 , L_2 and L_3 where L_1 , L_2 and L_3 are edge lengths related to the burned out areas as shown in Figure 10. Let us take L to be the average of these three edge lengths

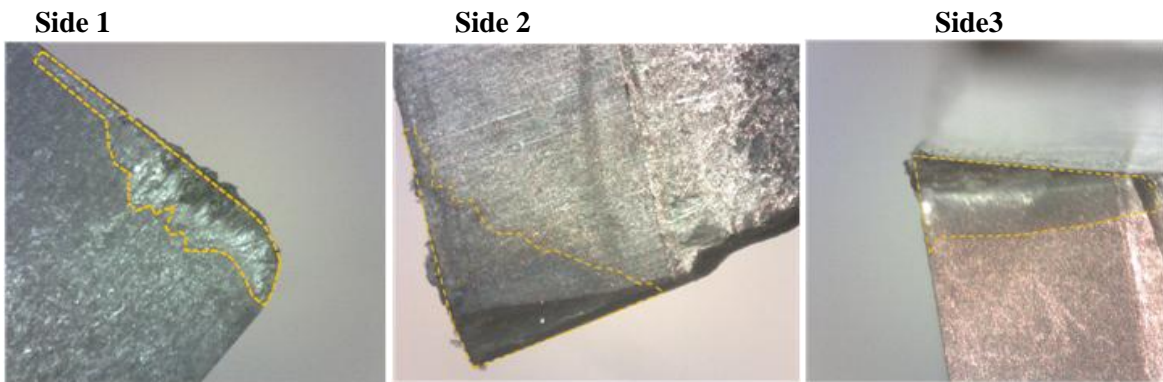


Figure 9. The burned-out area discoloration and contrast change as detected for three sides of an uncoated tool

$$L = (L_1 + L_2 + L_3)/3$$

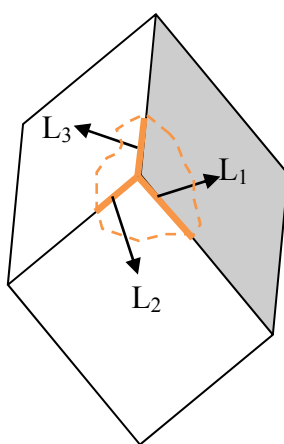


Figure 10. Schematic diagram showing the definition of length scale estimation

By finding the corresponding S/V ratio for the average length L from the graph in Figure 8, we define an index of conversion α to be the ratio $\alpha = S/V$ corresponding to L. Burned out volume $V=S/\alpha$, where S is the measured total surface area from the optical microscopy.

3.4 IN HOUSE THERMAL CYCLING TEST FACILITY

To evaluate aluminum die casting coatings, we designed an automatic in house metal dissolution/thermal cycling test setup. Figure 11 shows the thermal cycling test facility comprised of (a) the core pin handling arm and control board, (b) furnace for aluminum melting, (c) water quenching bath. This set up was used to transfer coated specimen between molten Al and water repeatedly creating the thermal cycling stress in the coating. We have tested our novel coating in this setup in comparison with TitanCoatTM coating. The difference between the initial weight and the weight after test is noted for each pin. After this, each pin is sectioned to characterize the thermal fatigue cracks under SEM.

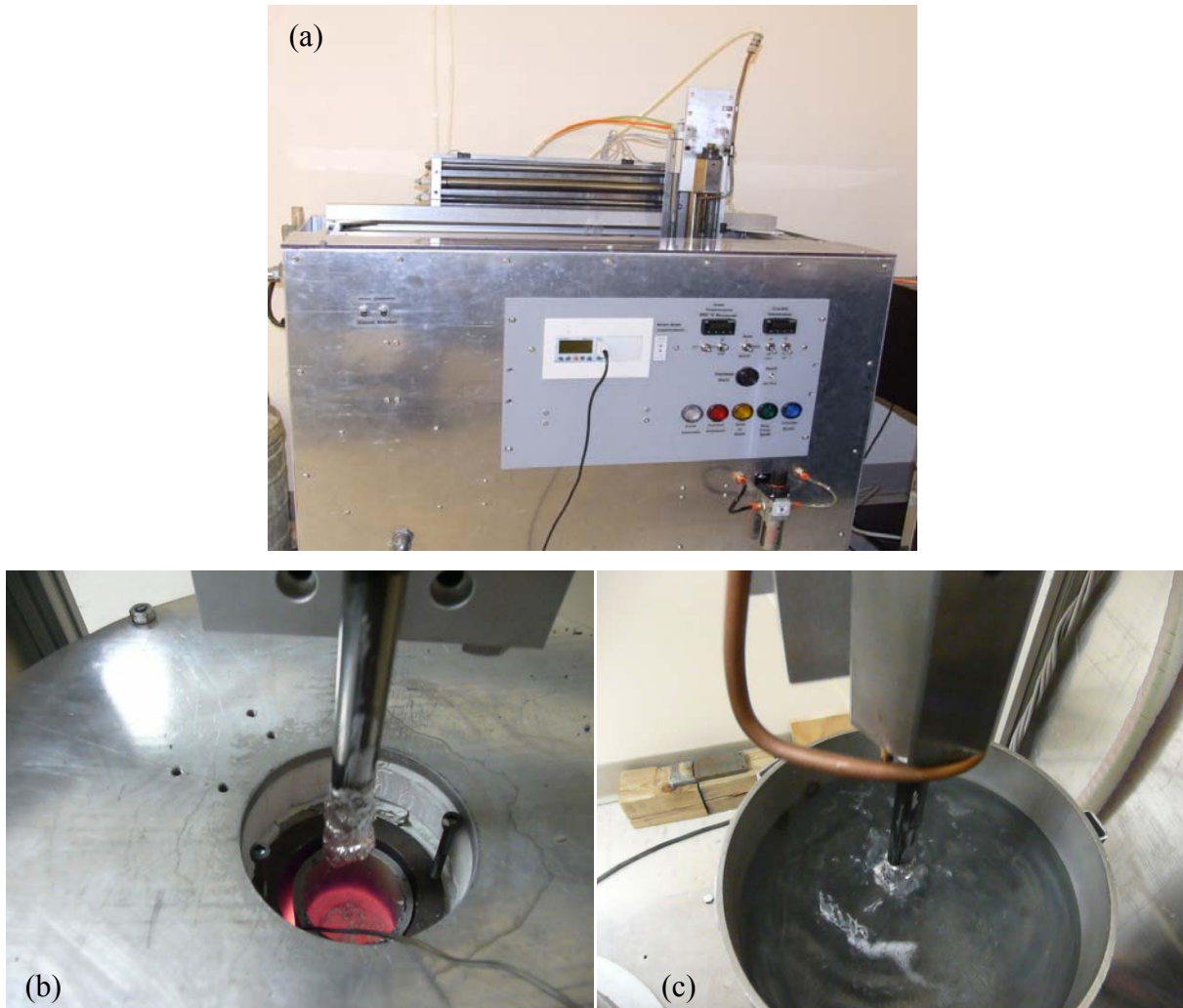


Figure 11. (a) Control board and mechanical arms (b) Molten Al bath (c) Cooling water reservoir

4.0 **RESULTS AND DISCUSSION**

In this section, we describe results for coatings in two major categories. 1) Cutting Tool coatings and 2) Die casting Tool coatings. In both of these categories, we have evaluated the coatings with our in-house facility and through our industrial partners. The results of these characterizations are presented below.

4.1 CUTTING TOOL COATINGS

One of the significant accomplishments achieved in this project is a novel cutting tool coating (GreychoTM) that is conformal with complex contour of the cutting tools and brought significant improvement to tool life (almost 6 times!) as reported by Triangle Precision from their commercial use. We applied our in-house evaluation technique (optical microscopy of tool surface degradation pattern (see Section 3.3)) to study the performance of these tools before we sent them to Triangle Precision and Kapex Manufacturing. Results from this analysis are described in the following section.

4.1.1 **In House Study**

For this study, we used triangular cutting inserts described in section 3.2. These cutters were coated with three different coatings, Greycho ITM, Greycho IITM and a novel CVD coating (BrochoTM). The performances of these cutters were compared to that of an uncoated cutter. After the cutting procedure explained in the experimental section, the burned out volumes of these pieces were evaluated and compared.

Figure 12 shows the cutting related discoloration (burned out area) and contrast observed from optical micrographs of Greycho coated tool tips along with the base line. As we can see, the discolored area for Greycho coated tools is significantly lesser than that of the uncoated baseline tool. The actual areas for these tools were calculated from these figures and burned out volumes were computed as described in Section 3.3.

Results of these measurements are shown in Figure 13. From Figure 13 it is evident that tool with Greycho-IITM coating has least wear-burned volume or better protection for the tool than Greycho-I. The uncoated tool got the maximum burned-out volume. The performance of BrochoTM coating fell just above the uncoated cutter (or baseline).

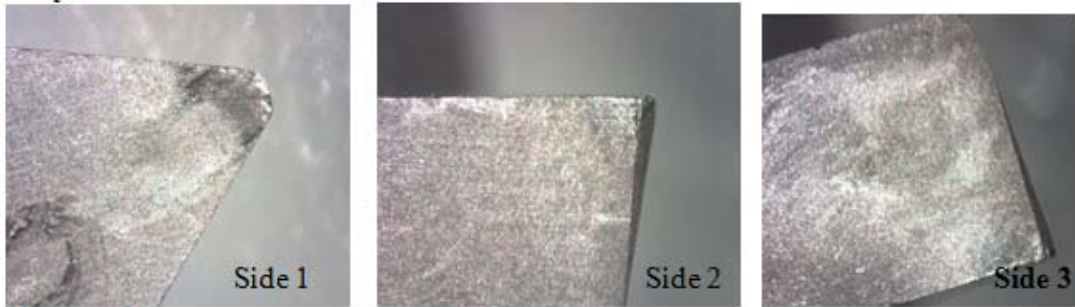
Greycho-I**Greycho-II****Baseline**

Figure 12. The burned-out area discoloration and contrast change as detected for three sides of each Triangular inserts used for coating evaluation

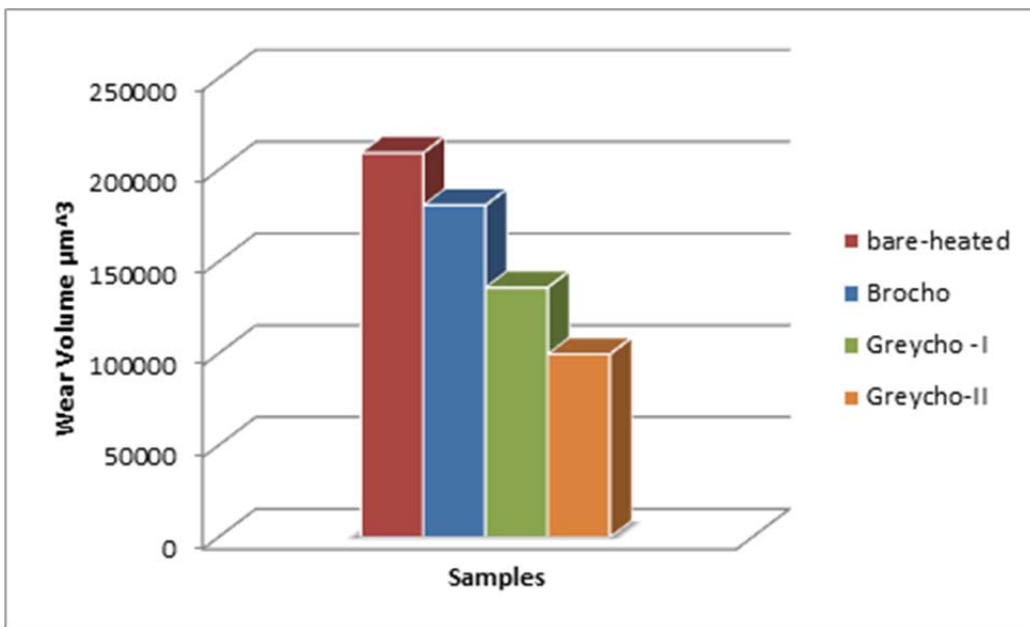


Figure 13. Total burned-out volume of various coatings compared to uncoated sample

4.1.2 Industrial Level Study

(a) *Triangle Precision*

During this project Triangle Precision provided numerous tools to UES for coating evaluation. These tools were coated with various experimental coatings that protected these tools at different machining situations. We describe here results from one of these set of coatings used for deep roughening of hard steel. Figure 14(a) shows the cutting tools as we received them. The corresponding numbers shown under each tool in the figure specifies tool types. These tools are uncoated as we received them. The tools were coated with our novel Greycho I TM, Greycho II TM and a TiN based conventional tool coating. Figure 14(b) shows Greycho II TM coated tools.

After the coating, they were given back to Triangle to evaluate their performance. They used these tools in their industrial cutting applications and came up with a performance comparison with commercially coated tools used in the same machining conditions. The tool life was measured by number of pieces machined. The results are given in Figure 15, showing the coating type and the tool type (on the top of the bars). From the evaluation results provided by Triangle Precision, it is evident that UES coatings' overall performance was very good compared to standard TiN coating. GreychoTM -II fared very well compared to other two on both cutting tool types and different cutting environments. On the tool type 1212, (3/8 inch round head end mill) GreychoTM -II coating fared significantly better than commercial coating, almost 6:1 ratio. Coating GreychoTM -I also could outperform commercial coating to a certain extent for small tools. However, the performance was not appealing like that of GreychoTM -II. The performance of TiN coating was poor compared to GreychoTM -I, GreychoTM -II or commercial coating. Presently we are working on GreychoTM -II coating optimization and the overall performance.

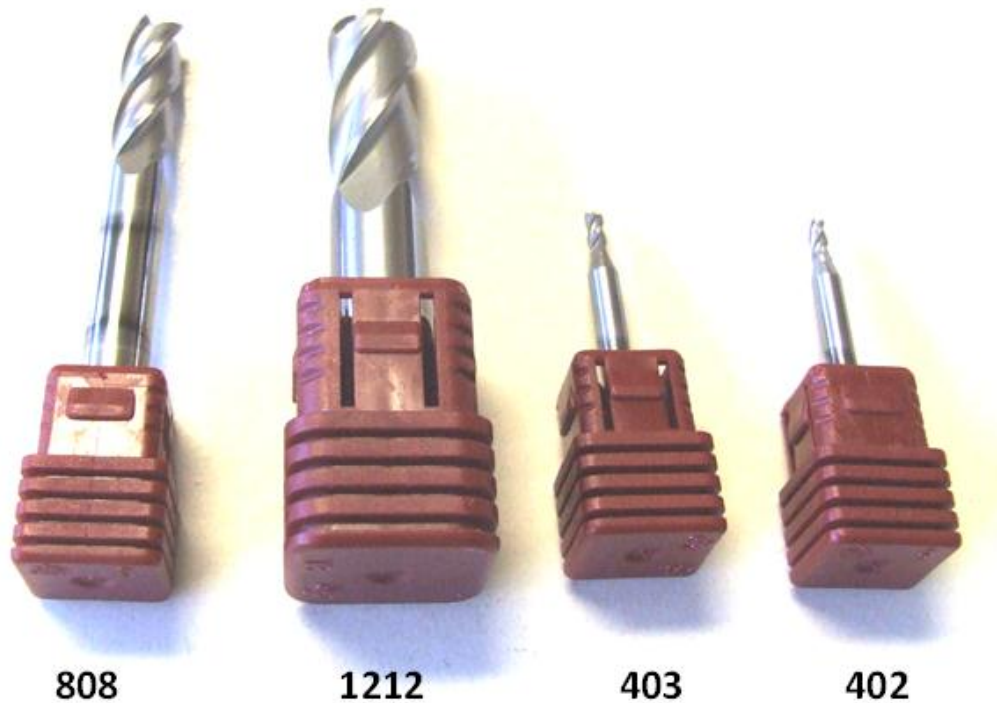


Figure 14(a). Uncoated Carbide Cutting tool received from Triangle Precision that are used in steel machining (lower numbers designates the tool type)



Figure 14(b). Carbide Cutting tool coated with Greycho II TM coatings provided to Triangle Precision for steel machining.

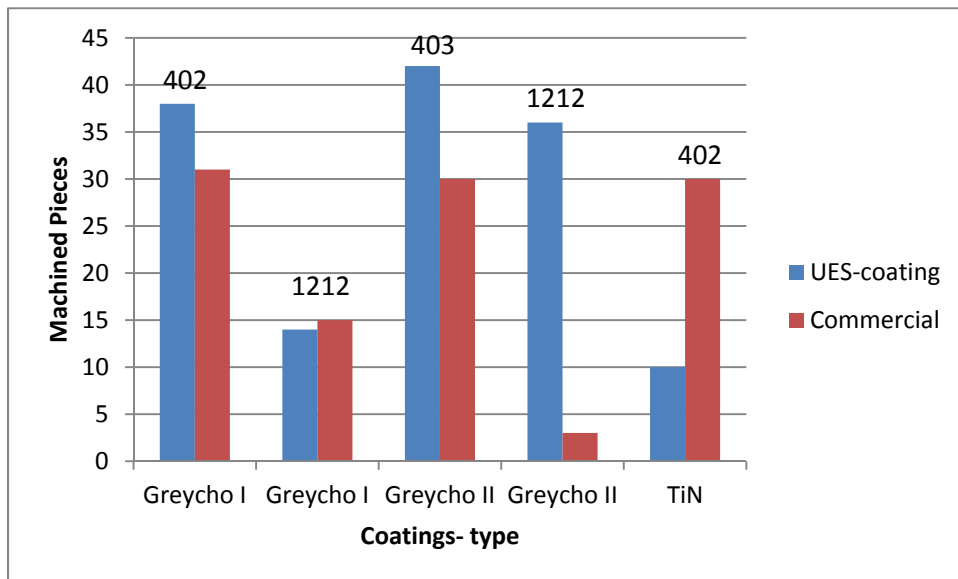


Figure 15. Coating performance, UES vs. Commercial coatings (Triangle Data)

(b) Kapex Manufacturing

Kapex, the second industrial partner provided us with cutting tools as well as parts used for aluminum die-casting. The cutting tools were coated with Greycho II™ coating with a new bond-coat to suit the application and delivered back to them.

Figure 16(a) shows the uncoated carbide roughening end mills, their workhorse, used in hard steel machining. These tools were coated with Greycho II™ coating (Figure 16(b)). They rough machined an entire set of rotors with these tools with very aggressive passes. The cutting parameters used for this work is given below in Table 2.

Table 2. Cutting Parameters

Work material - H13 RC 25
 Cutting time – 12 hours.
 Depth – Two spiral cuts of 0.75" (1.5")
 RPM – 7300 Dry
 Spiral speed – 270" per min.

The standard tool they normally use that has a commercial coating on it became unusable after two passes. UES coated tools were in excellent shape even after the full machining of a rotor disc, which needs almost four passes to finish. They have looked at the tips and edges of the flutes under the microscope and found to be still in very good condition. The results are shown in the Figure 17(a). The tool in the picture was already used to finish three rotors. The coating material system we provided to Kapex seems to be very good for extending the tool life in rough cutting of hardened steel. They have provided us with data for commercial tools too. Figure 17(b) shows the performance of commercial tools. These discs are made of H13 hardened steel with a Rockwell C hardness of 25.



Figure 16(a). Uncoated Carbide Cutting tool received from Kapex that are used in hard steel machining.



Figure 16(b). Modified Greycho™ coated Carbide Cutting tool provided to Kapex that are used in hard steel machining.

Comparing Figures 17(a) and (b), the commercial tools used for only four hours withered and failed due to the excessive wear at the cutting edges and uncontrolled chemical wear adhesion at the flutes whereas Greycho II™ coated tools were sharp even after twelve hours of use.

Kapex sent us the used UES coated tools along with the used commercial tools for further analysis. They also provided us chipping from these tests collected at different intervals of the machining.

Figure 18(a) and Figure 18(b) show the optical micrographs of a used tool, which were coated with Greycho II™ and a commercially coated tool respectively. The commercial tool is used only for 1/3 duration of cutting time compared to the UES coated tool. It can be seen from the figures that UES coated tools are almost intact while the commercial tools were damaged and not usable. Table 3 shows the tool wear area for each flutes of typical tools tested. It can be seen from the Table that UES coated tools have minimum wear compared to commercial tools. In addition, second-generation coatings from UES out passed the first generation performance significantly.

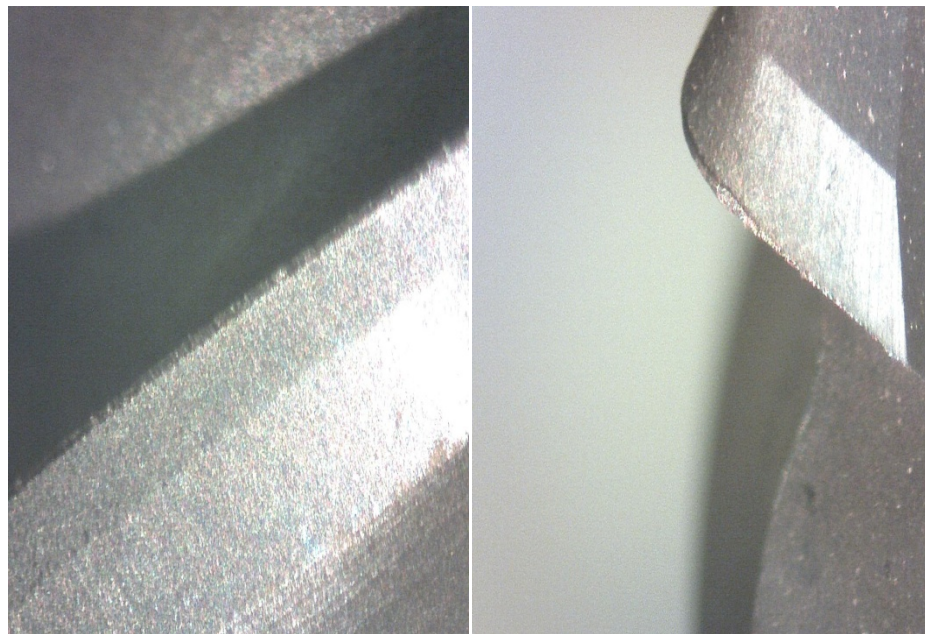


Figure 17(a). Digital micrographs of tools provided to Kapex after 12 hours of severe roughening



Figure 17(b). Digital micrographs of commercial tools after 4 hours of severe roughening



Figure 18(a). Digital micrographs of flutes showing cutting edges coated with Greycho IITM



Figure 18(b). Digital micrographs of flutes showing cutting edges coated with Commercial coating

Table 3. Wear area of tools coated with UES and commercial coatings

Greycho I		Greycho II	Commercial
Flute #	Area	Area	Area
1	5056	533	8751
2	1953	256	2519
3	759	398	11017
4	2407	392	18180
Mean	2543.75	394.75	10116.75
1	2304	1638	8996
2	4793	2355	3305
3	1512	2296	3379
4	2925	926	2866
Mean	2883.5	1803.75	4835

Figure 19 shows the overall performance comparison of UES coated tool compared to commercial coatings based on the data given in Table 3. In the plot, the average wear loss for the commercial coating is normalized and wear losses for UES coated tools are scaled accordingly. In a way, it can be seen that the Greycho II TM coating performed almost six times better than the commercial coatings. It is worthwhile to note that the Greycho coatings provided to Triangle Precision also came across the same ratio for the performance improvement for their roughening application.



Figure 19. Performance of UES coated Kapex tools compared to commercial coatings

After this, Kapex gave us a batch of similar end mills. UES developed a batch process that can successfully incorporate the novel coating onto this batch of twenty end mills. UES developed a process to coat the batch in a single run and the novel coating was uniformly deposited on all tools. Presently Kapex is using these tools in their day-to-day use.

4.1.3 Cutting Chips Study

Another interesting way to analyze cutting performance of tools is to look at the chips formation during cutting. Depending on the cutting nature of edges, the chips can have different geometry. Because of this, if we collect chips formed during different intervals into cutting, we can find out the evolution of cutting-edge geometry and the nature of temperature variation at the cutting edge.

Figure 20 shows the optical micrograph of multiple chips collected almost four hours into cutting from commercially coated tool (Figure 20(a)) and chips collected from Greycho II TM coated tools in (Figure 20(b)). As we can see chips formed of commercial tools is all broken down into tiny fragments with irregular shapes while Greycho II TM coated tools chips are elongated up to 2-3 cms. This shows the bluntness of commercial tool after four hours of use while Greycho II TM coated tools remain sharp and form long regular elongated chips. Another interesting property of the chip is the number of twist we observe on a single chip and overall color of the chip. As the sharpness of the tools diminishes, the chips formed get more stress during the separation process and get highly plastically deformed (more twists formed) produces more heat and are darkened in color. In the case of sharp tools, all these effects are minimized and chips remain shiny and less deformed. Figure 21 shows the optical micrograph of a single chip collected almost one hour into cutting from commercially coated tool (Figure 21a) and a single chip collected almost ten hours into cutting from Greycho II TM coated tools (Figure 21b).

As we can see chips formed from the commercial tools were darkened and were twisted more into the first hour of cutting while Greycho II TM coated tool produce chips with shiny surface and minimum twists even after ten hours of use. This substantiates the superior performance of Greycho II TM coated tools, which we assessed from the wear area computation made on each flutes and cutting edges reported in the last section.

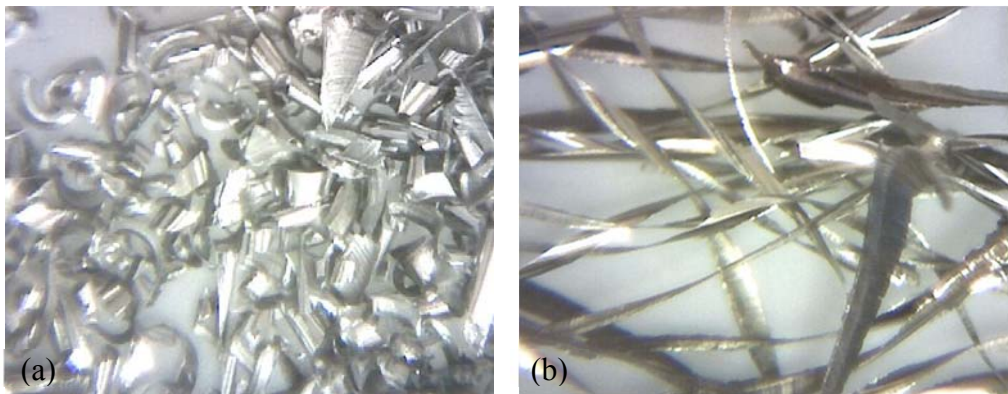


Figure 20. (a) Optical micrograph showing chips (4 hours) collected from commercially coated tools and (b) Optical micrograph showing chips collected (12 hours) from UES coated tools



Figure 21. (a) Optical micrograph showing single chip (one hour) collected from commercially coated tools and (b) Optical micrograph showing chips collected from UES coated tools (ten hours)

4.2 DIE CASTING COATINGS

The other significant accomplishment achieved during this project is a novel die casting coating, Titan Generation II TM, which is temperature resistant, well-adhered dense film, which brought significant improvement to die casting tool as reported by Honda Manufacturing from their commercial use (See Table 4). We applied our in-house evaluation technique (Thermal cycling facility) to study the performance of these tools before we sent them to Kapex Manufacturing (see Section 3.4). Results from this analysis are described in the following section.

4.2.1 In House Study

We have developed mainly three different coatings for die casting application. They are Titan Generation I (B), Titan Generation I (modified) (C) and Titan Generation II (D). Titan Generation I and Titan Generation I (modified) are just optimization of the chemical phase mixing of our old material system (TiN). However, Titan Generation II is based on HfB₂ and used a new processing technique to form it. These coatings can prevent these tools from metal dissolution, aluminum soldering, and corrosion and wear from repeated thermal cycling. To evaluate the performance they are tested in our own dip testing-thermal cycling facility. As an overall evaluation, weight change and the surface defects observed in dipped region were noted as preliminary parameters. The uncoated pin underwent maximum weight change and some unwanted tiny patches at the dipped region while both coated specimens got practically no weight change. The TitanCoat TM coated sample is better than uncoated sample while the newly developed Titan Generation II TM coating behaved much better than other samples.

4.2.2 Failure Analysis of Core Pins

A thorough investigation into the performance of our three coatings is made as follows. The test bars were placed into molten aluminum held at 750°C and transferred to water reservoir for cooling. The holding time can be varied in both of these reservoirs. We chose 4 sec, for Aluminum bath and 6 sec. for water bath per cycle. Generally, this method is used to test the service life of the various coatings on H-13 bars and to evaluate the dissolution rate of coated pins compared to uncoated pins. The bars were tested for various cycles in steps of 800 cycles. This process was repeated for 7800 cycles for all these coatings, to collect enough data to evaluate the dissolution rates of alloy. Following sections 4.2.3 to 4.2.6 describes the results of this study.

4.2.3 Optical micrograph Surface Study

Figure 22 shows optical micrograph of the thermally cycled surface of coated test bars. The less-reactive ceramic coatings (TiN, HfB₂) provides a mechanical barrier to protect the H-13 steel from contacting the reactive molten aluminum alloy. In other words, the soldering reaction could not take place if the coating remains intact over the surface of the H-13 matrix. Figure 22 clearly shows the surface defects formed by soldering for various coatings tested, which also depicts erosive pits, minor cracks or delamination of the coatings.

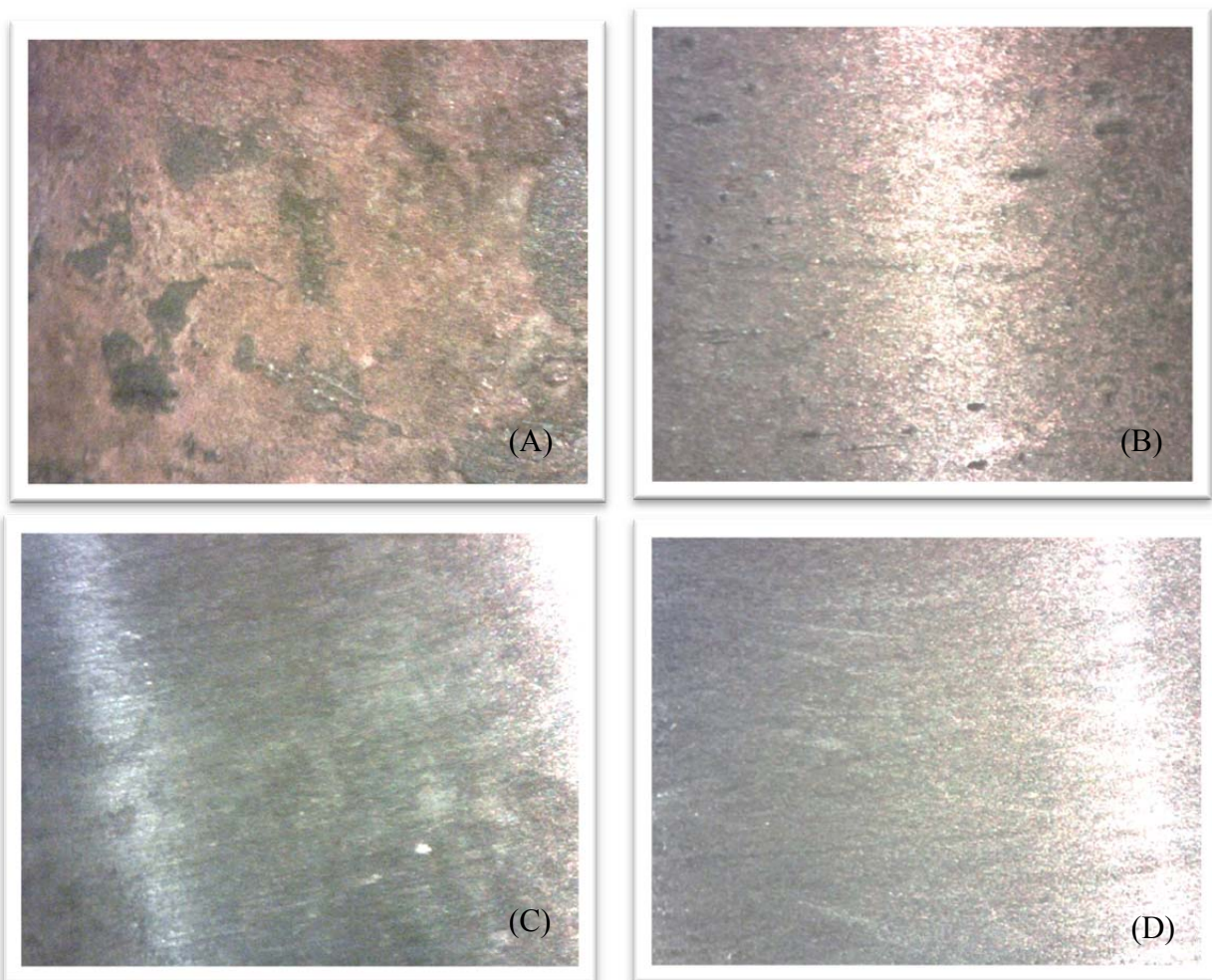


Figure 22. Optical micrograph (50X) of the thermally cycled surface coated with (A) Uncoated pin, (B) Titan Generation I coating, (C) Modified Generation I coating, and (D) Titan Generation II coating

As we can see, these coatings can protect the pins at different levels as the damage of the surface is decreased from sample A (uncoated) to Sample D (Titan Generation II TM). Sample A, the uncoated sample shows significant damage and aluminum soldering and surface cracks. The crack of coating could be seen clearly in these images except sample D. Two typical failure modes were cracking and detaching from the H-13 surface. The differences in mechanical and physical properties will cause the coating and the H-13 to expand and contract at different rates during the die casting thermal cycle. During the die casting process, the molten alloy is injected at high temperature, high speed, and high pressure, which will quickly heat up the core pins. When the die opens, the core pins quickly cool back down. These cyclical temperature and pressure changes cause alternating and different deformations in the coating and the matrix, leading to both thermal and mechanical fatigue of the bonding layer at the coating/steel interface if the core pin experiences hundreds or thousands shots. In addition, the high-speed (70 m/s ~ 100 m/s) molten alloy could easily wash the detached coating away during the die filling process. If a coating failure occurred, either because of cracked coating or detached coating, the failure site would become a solder generating area, and the reactive molten alloy could react directly with the H-13 matrix. As we can

see from the surface microscopy, the sample D, which is coated with Titan Generation II TM coating shows no damage

To better understand the degradation process, these core pins were analyzed in detail. It was found that the progression of soldering on the core pins from beginning, through the final growth and development could be divided into different steps: namely local coating failure, pit formation, in-depth growth of a pit.

4.2.4 Local Coating Failure

The samples with coatings can still be damaged from casting process. Some defects, such as coating non-uniformity, coating micro cracks and discontinuity, could not be avoided. Second, the physical properties of the coating and H-13 matrix are quite different, especially the ductility, thermal conductivity, and coefficient of thermal expansion. Concentrated local defects like this can affect the performance of the coating.

4.2.5 Pit Formation

When the molten aluminum contact with the H-13 matrix, solder formation starts a pit on the surface of the H-13 matrix. Figure 23 shows the scanning electron micrographs of the cross sections of these samples cut at the bottom of the dipped region. Specimens were prepared for microstructure analysis for SEM with EDS. All the specimens were mounted in epoxy, which can better support the coatings and adhesive soldering materials. These specimens were ground and polished following the standard metallographic procedures.

Figures 23(a) and 23(b) shows the micrographs for the cross section of uncoated specimen at two different magnifications. There are numerous pits formed on the surface showing the vulnerability of bare H-13 steel to molten aluminum. These pits starts as small areas and grow around 20~30 microns laterally and 50~60 microns in depth. At this level of soldering, it can be seen that the Al-Fe reaction area grew into the H-13 matrix as well as outward from the core pin. The shape of pit in the H-13 matrix appeared conical. The growth rate in lateral direction was slower than the radial direction. As the pit grew, it changed from a hemispherical to an elongated conical shape. The lateral growth of the reaction area led to the further degradation failure. Figures 23(c) and 23(d) shows the cross sections of the pin coated with Titan Generation I TM coating. Comparing same 200 μm scale pictures it is evident that Titan Generation I TM coating could reduce the pit formation significantly in H-13 steel substrates. In more magnified Figure 23(d), we see a region on the periphery where steel surface is damaged and coating detached from the surface. Fragments of the failed coating could be found in the aluminum side of the reaction area, outside the pit. In Figure 23(e), we see the cross section of a pin coated with modified Titan Generation I TM coating. We do not see much pitting into the substrate yet. The surface defects exhibited in the optical micrographs were considered due to local coating imperfections. These surface defects were originated by cracked coating or discontinuities in the coverage as we see in the magnified picture Figure 23(f).

Figures 23(g) and 23(h) shows the cross sections of the best performing coating. As we can see, this coating (Titan Generation II) is protecting the steel at 7800 dips without much damage to the surface. The H-13 steel rod surface is intact, and the coating remains without any crack or delamination even in the highly magnified picture in Figure 23(h).

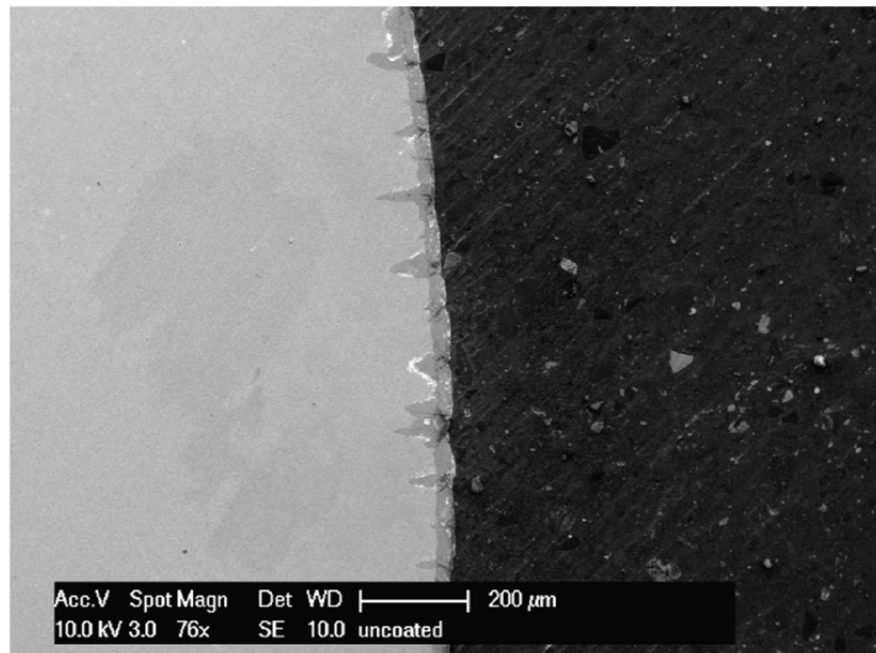


Figure 23(a). Cross section of uncoated pin showing numerous pits formed into the H-13 substrate.

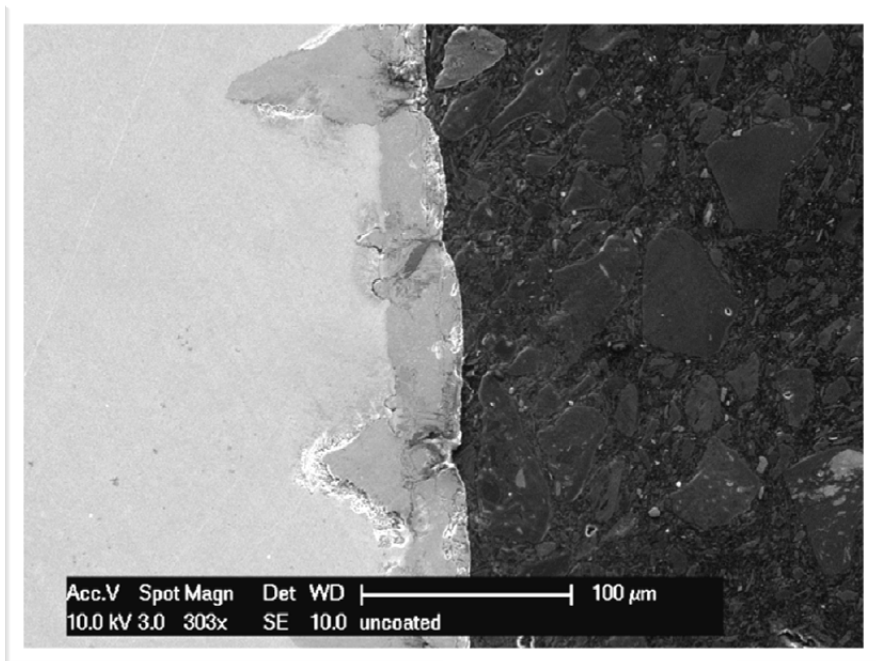


Figure 23(b). Cross section of uncoated pin showing the detailed structure of pits

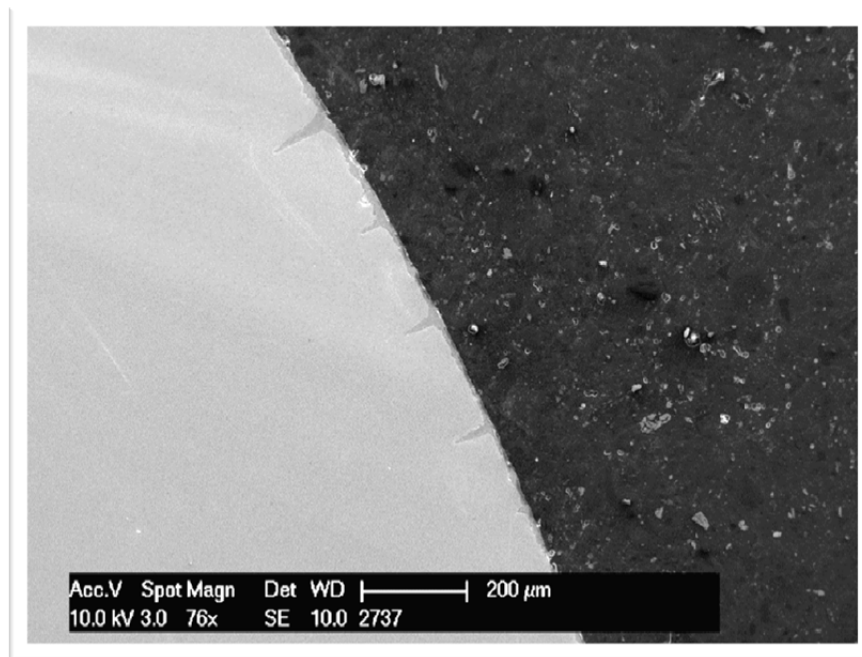


Figure 23(c). Cross-section of Titan Generation I coated pin showing failure of the coating and pits

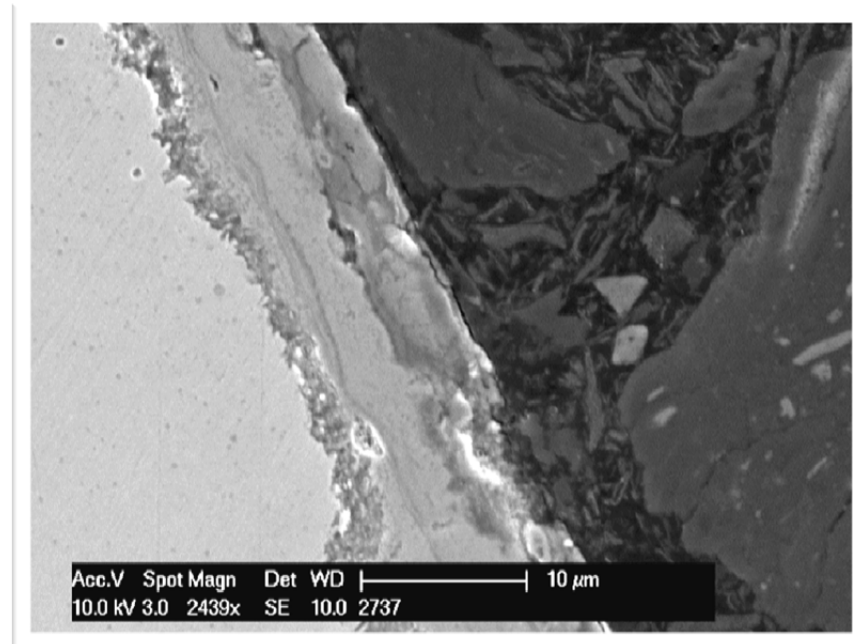


Figure 23(d). Magnified cross-section of Titan Generation I coated pin showing delamination of the coating and steel surface degradation.

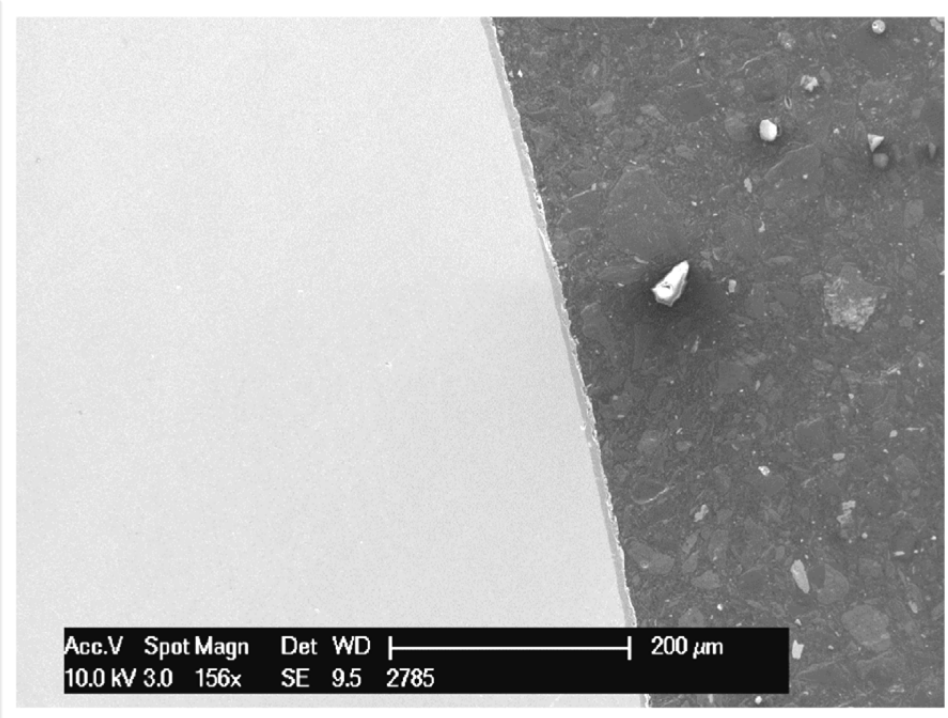


Figure 23(e). Cross-section of modified Titan Generation I coated pin showing overall performance

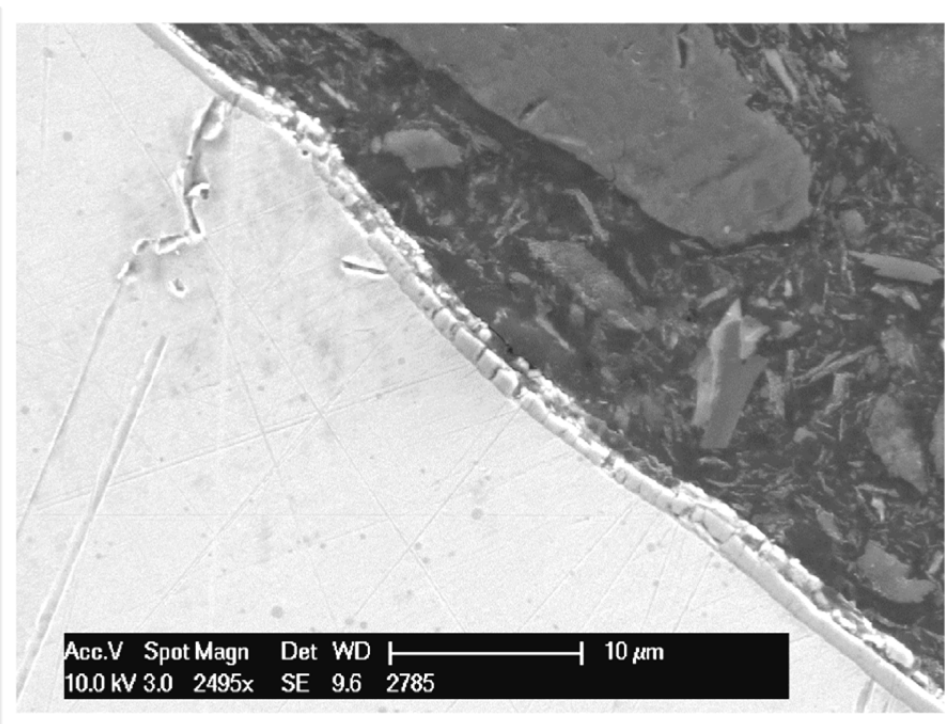


Figure 23(f). Magnified cross-section of Titan Generation I coated pin showing delamination of the coating and steel surface degradation.

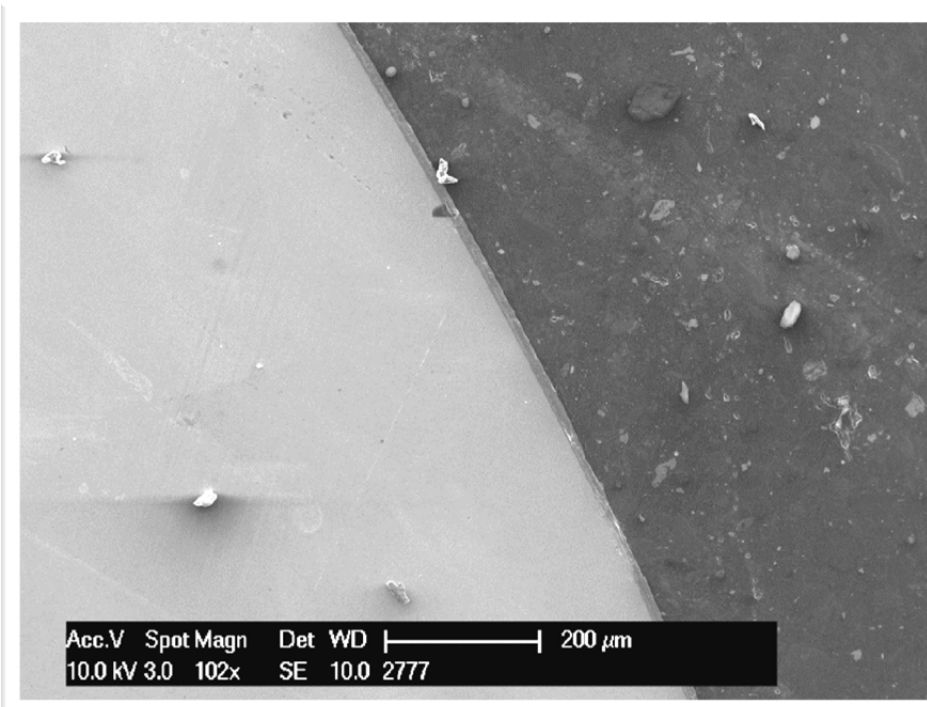


Figure 23(g). Cross section of Titan Generation II coated pin showing undisturbed coating and steel surface.

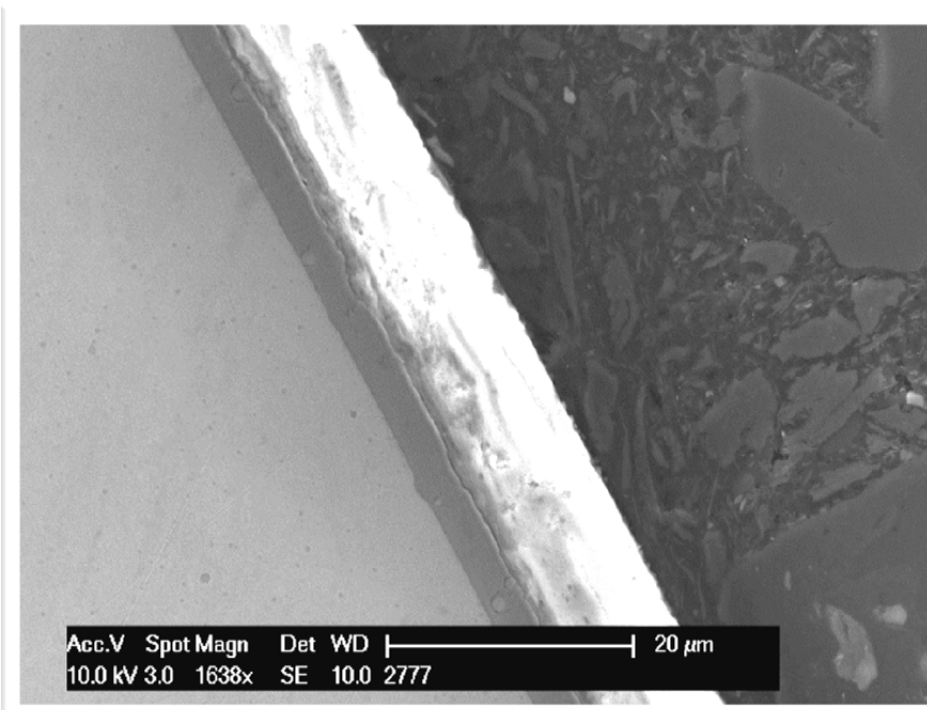


Figure 23(h). Magnified cross section of Titan Generation II coated pin showing undisturbed coating and steel surface.

4.2.6 In-depth Growth of a Pit

After a pit or solder reached a lateral growth of 40 to 60 microns, the in-depth growth began to accelerate and turned the pit into a parabolic/pyramidal shape while the lateral growth continued to destroy the remaining coating. In the magnified picture of the Titan Generation ITM coated pin, Figure 23(d), the damaged coating, damaged H-13 matrix periphery, and the reacted area are all shown clearly. The coating appeared to protect the matrix in the non-soldered area, yet disappeared in the soldered area.

Figure 23(b) shows the typical image of the soldering area (with 60 microns in lateral direction and 90 microns in depth), which contained the Al-Fe reaction area and the Al alloy area (the eutectic aluminum phase) located in the center of the soldered area. A 15-micron spot scan located in the reacted pit region (in Figure 23b) was used to analyze the elemental distribution of the pit. The graph in Figure 24 shows the atomic percentage of elements at the center of the reacted area. Al and Fe are the main component elements in this image besides oxygen. An important feature shown from this study is that the Al alloy region extends deep into the tip of the pit. Most likely, the Al eutectic phase in the Al alloy region became a liquid phase when molten aluminum heated up the core pin. Convection within the liquid phase accelerates the in-depth growth of the pit. The sharp tip of the Al alloy region also is an indication that the high pressure during the insertion stage of the pin into the molten aluminum alloy may have been transmitted through the liquid eutectic phase to tear the inter-metallic phase apart, forcing liquid to fill the crack thus formed.

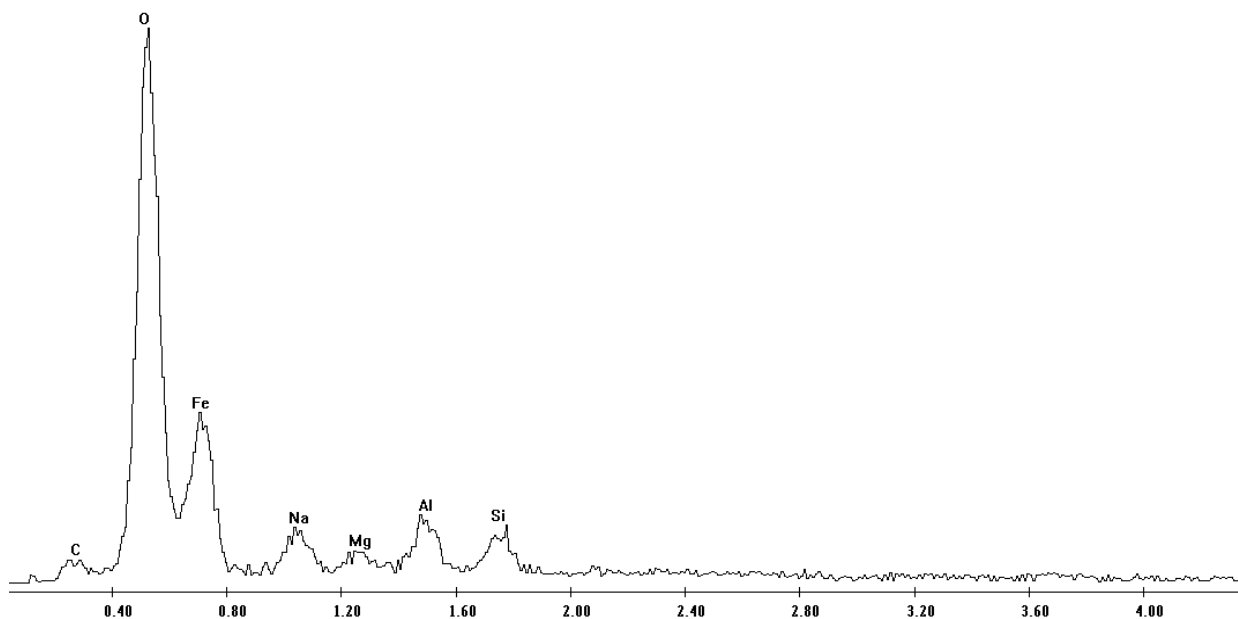


Figure 24. EDS data inside a pit showing the major elements (uncoated pin)

4.2.7 Titan Generation II Coating and TitanCoatTM

UES has been the Tier 1 supplier of molten aluminum corrosion resistant die casting coating to Honda of since 09/2006. We have been supplying TitanCoatTM coating for this purpose.

It is appropriate to have a direct comparison of TitanCoatTM and Titan Generation IITM coatings. These coating were applied to 6-inch H-13 steel pins and they were tested for aluminum dissolution and thermal cycling stress along with an uncoated pin in our thermal cycling test facility. Preliminary surface

changes from a 1000 cycle dip test are shown in Figure 25. The top picture shows digital photo of the rods after the dip. Bottom one-inch length was dipped into the molten aluminum. The dip cycle consists of 5 seconds in molten aluminum, transferred to room temperature water, dipped for 4 seconds. The temperature of the aluminum bath was held at 850 °C. From the overall look, the uncoated one is severely damaged and other two do not seem to have been affected much. The bottom frames of Figure 25 show the magnified surface morphology of each rod. The green rectangular regions shown in the top pictures are selected in the magnified pictures. It is evident from the pictures that uncoated bare rod under goes severe damage like pitting and eroding into the solid rod. TitanCoat™ coated sample shows only surface cracks that are less severe compared to uncoated baseline. Newly developed Titan generation II™ coated sample is showing minimal damage to the sample surface. No cracks seem to be penetrating into the solid body. To check this we have made cross sections of these rods at position shown by the horizontal arrow in Figure 25. The sections were mounted and polished to one-micron roughness and examined under scanning electron microscope (SEM). Figure 26 shows the results of this study. Figure 26(a), (b) and (c) show the bare, the TitanCoat™ coated and the Titan Generation II™ coated rods respectively. We purposely avoided the highly pitted area for the sectioning. From Figure 26(a) it is evident that aluminum is attacking solid rod after penetrating into it through surface cracks. From Figure 26(b), TitanCoat™ coated sample still keeps a slight portion of the coating even though the coating is partially detached by the aluminum. That gives protection to the substrate from the molten aluminum. Figure 26(c) shows the effect of Titan Generation II™ coating in protecting the substrate. As we can see, the coating is almost intact after 1000 dip cycles. Coating does not seem to be affected by the thermal stress cycles between the molten aluminum bath and the room temperature water. The substrate seems to be intact under the coating. It may take several more thermal cycles to observe some damage to this coating system.

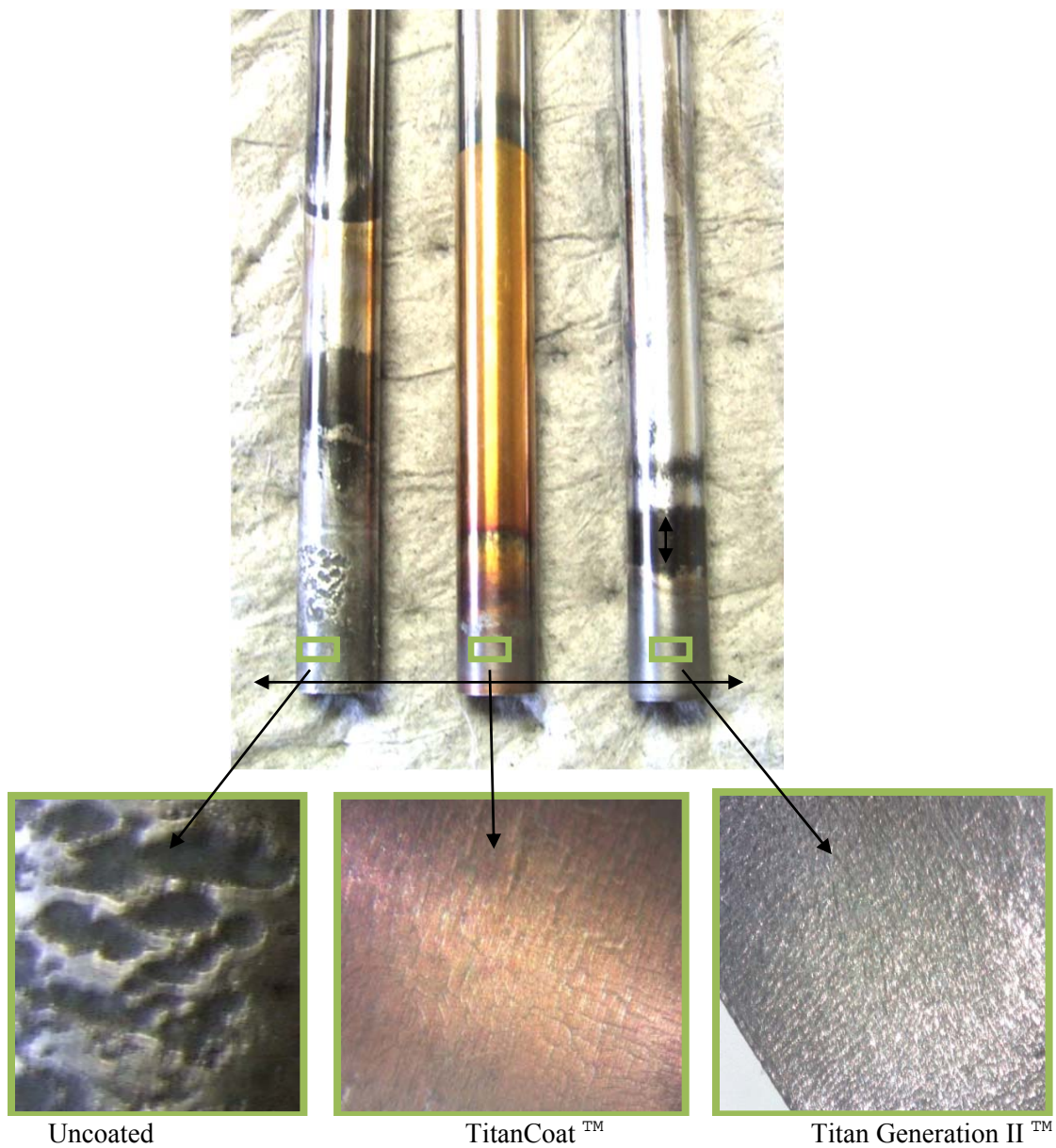


Figure 25. Metal dissolution/thermal stress dipping test results.

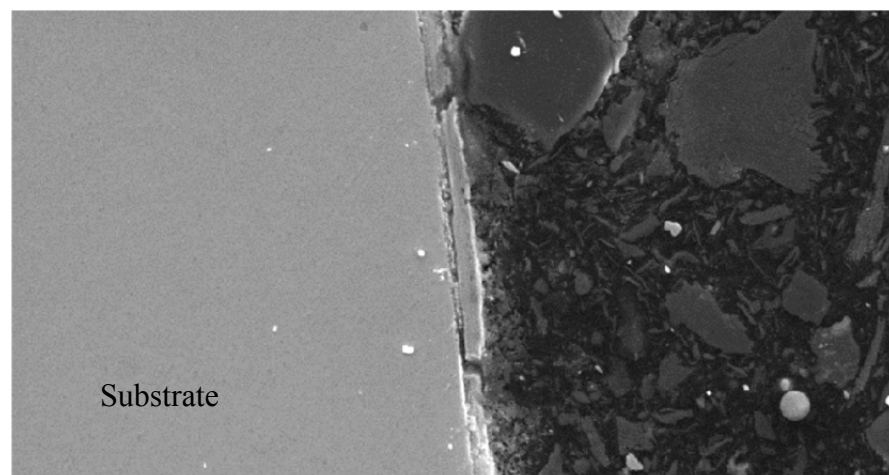


Figure 26(a). SEM micrograph showing X-section of bare rod

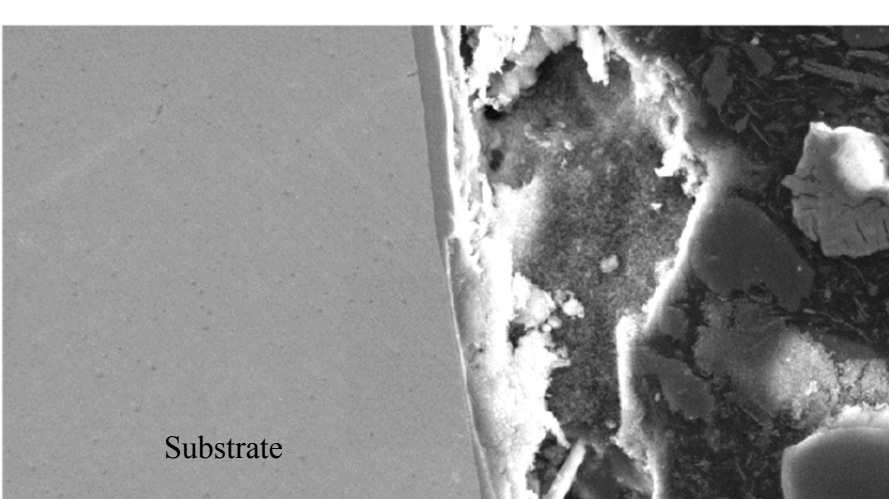


Figure 26(b). SEM micrograph showing X-section of Titan coated rod

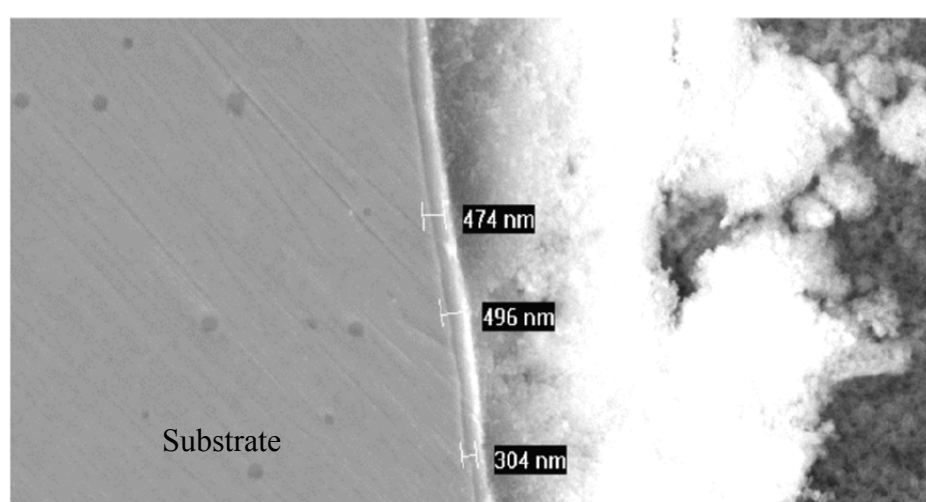


Figure 26(c). SEM micrograph showing X-section of Titan Generation II coated rod

4.2.8 Titan Generation II, Industrial Level Study

Honda of North America, Anna, OH sent us a number of pins through Kapex to be coated with our advanced coating for testing in their production. We provided them six Titan Generation II TM coated pins with three different bond coatings (bond coatings enhance the adhesion between the top functional coating and the substrate) (2 pins having the same bond coat). Table 4 shows the latest results of the in-plant tests conducted so far using these pins. (This has been an ongoing effort with Honda) One pin at the location C6 broke. However, that has nothing to do with the coating. The rest of the coated pins performed very well. They have already exceeded the standard cycle goal for V6 model and close to meeting the goal for R40 model. The coated pins were still in use at the time of this report.

Table 4. Record of Production Cycles using the Titan Generation II Coated Pins

Coating	Pin Location	Die # and model	Cycles	Std Cycle Goal	New Goal
Bond1- Titan Gen II	UB9	Die #7 V6	31809	15000	30000
Bond1- Titan Gen II	UB11	Die #7 V6	31809	15000	30000
Bond1- Titan Gen II	LB9	Die #7 V6	31809	15000	30000
Bond2- Titan Gen II	LB12	Die #7 V6	44039	15000	30000
Bond3- Titan Gen II	C6	Die #3 R40	12213	30000 broken	45000
Bond3- Titan Gen II	C7	Die #3 R40	44039	30000	45000
Bond3- Titan Gen II	C8	Die #3 R40	44039	30000	45000

As we can see from this data that die # 7 (V6 core pins) already surpassed their new goal for cycling and die #3 is only a few hundred cycles away from 45000-cycle new target which is 15000 cycles higher than the old standard goal. This data from the industrial use of our coating also confirms the result we observed from the in house metal dissolution/thermal cycling tests described in Sections 4.2.4-4.2.7.

4.3 ARGONNE NATIONAL LABORATORY COATINGS

4.3.1 Deposition System

The sputter ion plating system of ANL has been designed, built, and installed by the CemeCon-USA Co. under a CRADA supported by DOE-Office of Transportation Technologies. It has two independently controllable targets that can be made of Mo and Cu. In the presence of Ar+N₂ gases in the gas discharge plasmas, one can easily synthesize MoN-Cu coatings and deposit them onto various work pieces in its large deposition volume (typically 1 m³). Very high ionization efficiency of this deposition system insures pore-free (smooth) microstructure and strong adhesion between coating and substrate materials. Figure 27 shows the end mills and triangular cutters coated by this process.



Figure 27. End mills and triangular cutters coated with MoN-Cu using the sputter ion plating process.

4.3.2 Results

1) Rockwell C adhesion test

Adhesion of these films to the substrate was measured by Mercedes Rockwell C indentation method, a maximum load of 150 Kg is applied onto the coating and resulting indentation crater is studied for the mechanical characteristics of these coating. Figure 28 shows the micrographs for these indentation craters. As it is seen below, adhesion of the coating to substrate is rated as HF1 (very good).

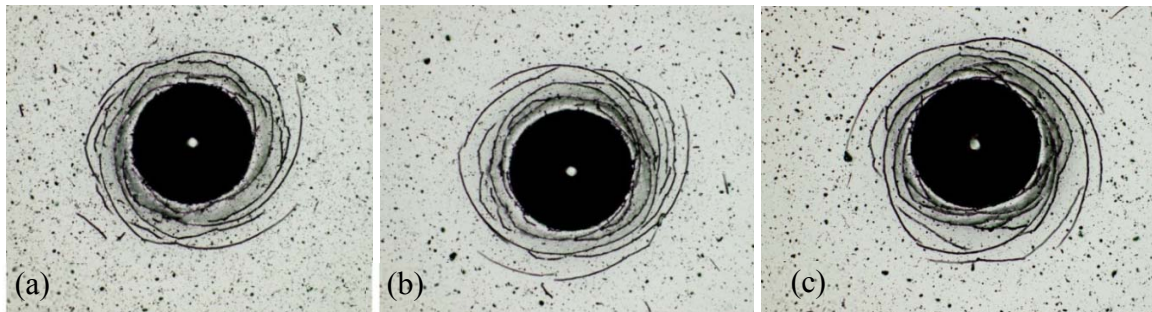


Figure 28. Rockwell C (a) middle, (b) 1st corner and (c) 2nd corner on steel witness

2) Tribological characterization of MoN-Cu flat vs 52100 steel ball

Friction and wear of these coatings are studied with a ball on flat tribometer. Following are the conditions used in this test. A $\frac{1}{4}$ " 52100 ball was used for this test. The normal load was set to 2N with a track diameter of 30 mm and 10 rpm resulting in a linear speed of 16mm /s. The relative humidity of the surrounding is held at 44% and the total run lasted for 1700 sec. completing about 285 revolutions per each run. This test involved no explicit lubricants. Figure 29(a) shows the friction trace from this test. The average coefficient of friction remained around 0.7 throughout the test. Figure 29(b) shows the wear scar of the MoN-Cu coated flat. Figure 29(c) shows wear scar profilometry of the flat with the line scan. The profilometry shows only nominal wear on the coated surface. Figures 29(d) and 29(e) show 3D-Wear scar profilometry of the ball and the ball micrograph respectively. It is evident from Figure 29(e) that the steel ball has significant wear at the contacting area.

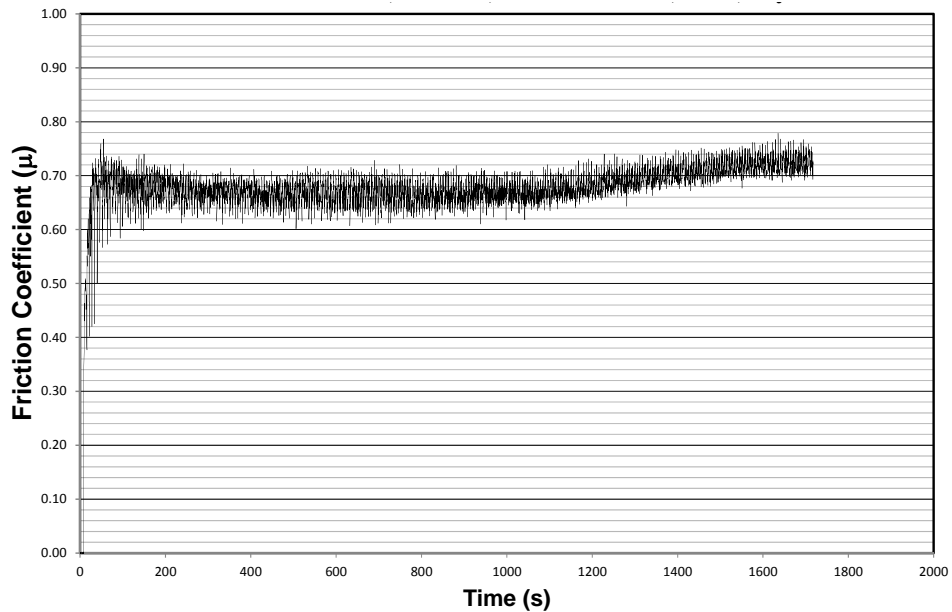


Figure 29(a). Friction trace, Friction coefficient Vs Time

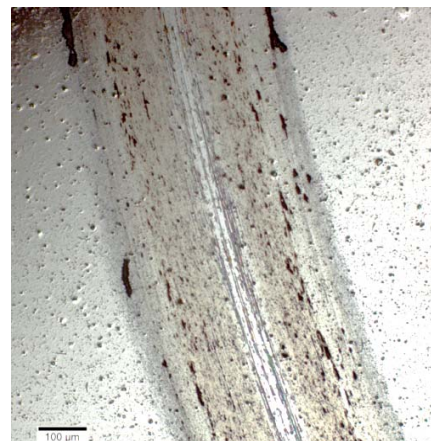


Figure 29(b). Wear scar of MoN-Cu flat

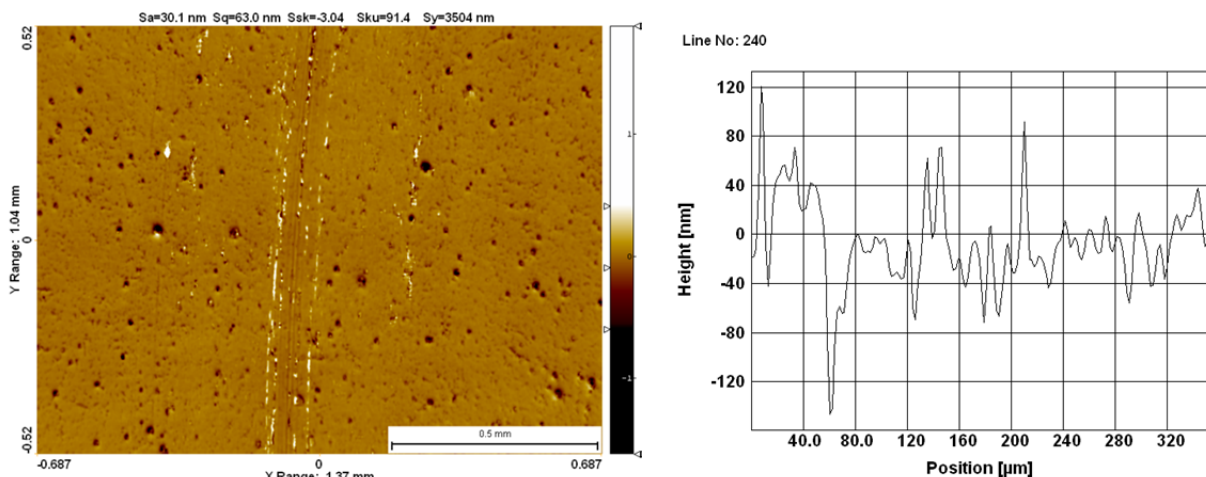


Figure 29(c). Wear scar profilometry of the flat with line scan

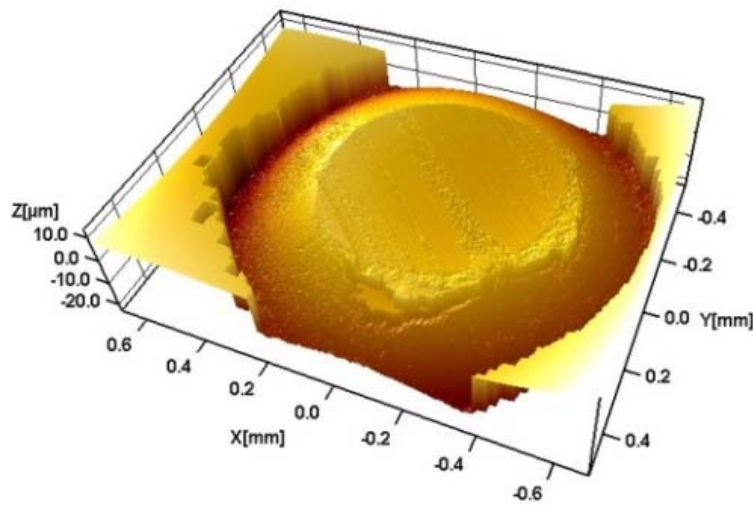


Figure 29(d). 3D-Wear scar profilometry of the ball

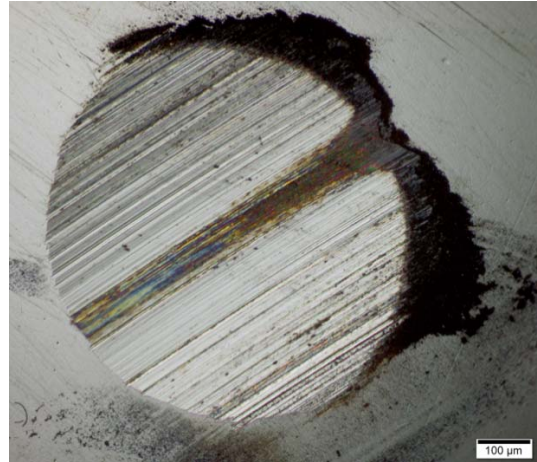


Figure 29(e). Ball micrograph

3) Tribological characterization of MoN-Cu flat vs Alumina ball

Friction and wear of these coatings are studied with a ball on flat tribometer. Following are the conditions used in this test. A $\frac{1}{4}$ " alumina ball was used for this test. The normal load was set to 2N with a track diameter of 26 mm and 10 rpm resulting in a linear speed of 14mm /s. The relative humidity of the surrounding is held at 44% and the total run lasted for 1800 sec. completing about 300 revolutions per run. This test involved no explicit lubricants. Figure 30(a) shows the friction trace from this test. The average coefficient of friction remained around 0.45 throughout the test. Figure 30(b) shows the wear scar of the MoN-Cu coated flat. Figure 30(c) shows wear scar profilometry of the flat with the line scan. The profilometry shows almost no wear on the coated surface. Figures 30(d) and 30(e) show 3D-Wear scar profilometry of the ball and the ball micrograph respectively. It is evident from Figure 30(e) that the alumina ball has no significant wear at the contacting area.

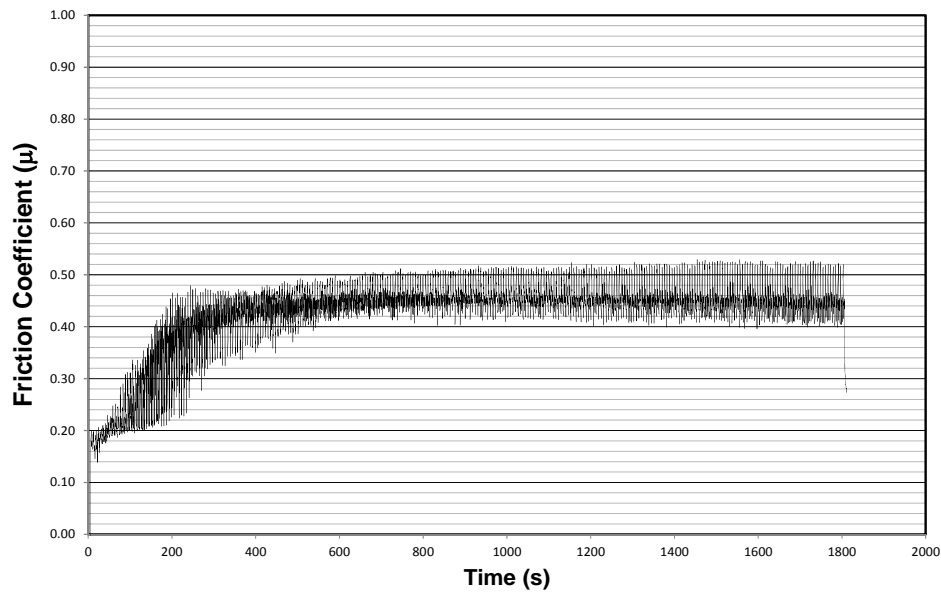


Figure 30(a). Friction trace, Friction coefficient Vs Time



Figure 30(b). Wear scar of MoN-Cu flat

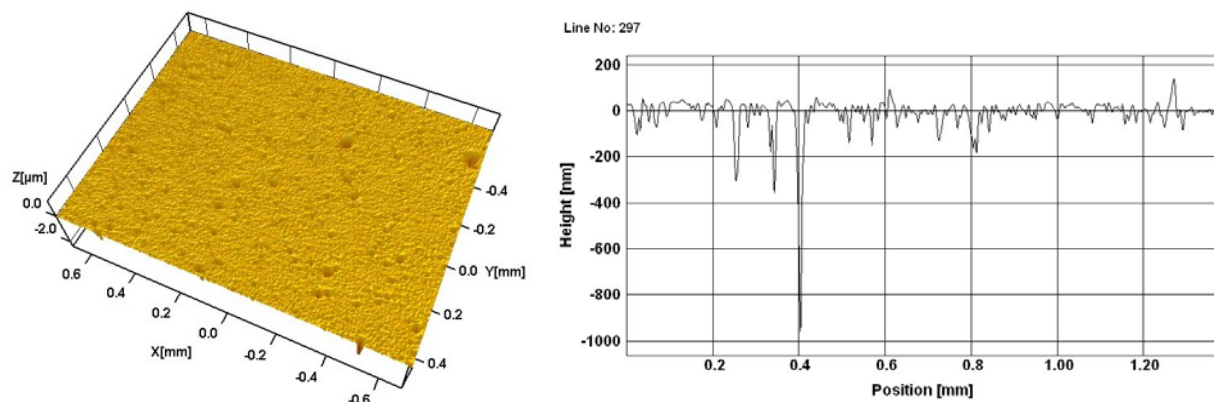


Figure 30(c). Wear scar profilometry of the flat with line scan

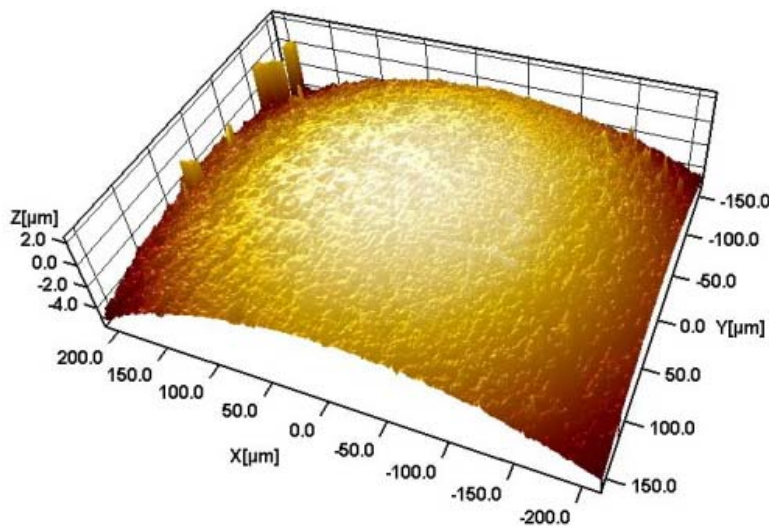


Figure 30(d). 3D-Wear scar profilometry of the ball



Figure 30(e). Ball micrograph

4) Tribological characterization of MoN-Cu flat vs 52100 steel ball with lubricant PA04

Friction and wear of these coatings are studied with a ball on flat tribometer. Following are the conditions used in this test. A $\frac{1}{4}$ " 52100 steel ball was used for this test. The normal load was set to 2N with a track diameter of 26 mm and 10 rpm resulting in a linear speed of 14mm /s. The relative humidity of the surrounding is held at 44% and the total run lasted for 1800 sec. completing about 300 revolutions per run. This test involved the lubricants PA04. Figure 31(a) shows the friction trace from this test. The average coefficient of friction remained around 0.12 throughout the test. Figure 31(b) shows the wear scar of the MoN-Cu coated flat. Figure 31(c) shows wear scar profilometry of the flat with the line scan. The profilometry shows almost no resultant wear on the coated surface. Figure 31(d) and Figure 31(e) show 3D-Wear scar profilometry of the ball and the ball micrograph respectively. It is evident from Figure 31(e) that the steel ball had significant wear at the contacting area.

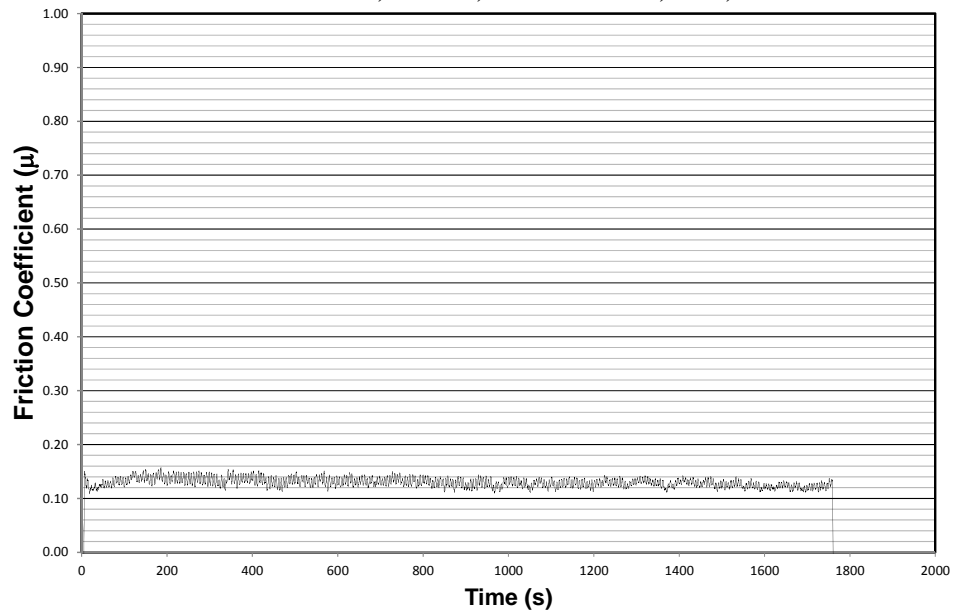


Figure 31(a). Friction trace, Friction coefficient Vs Time

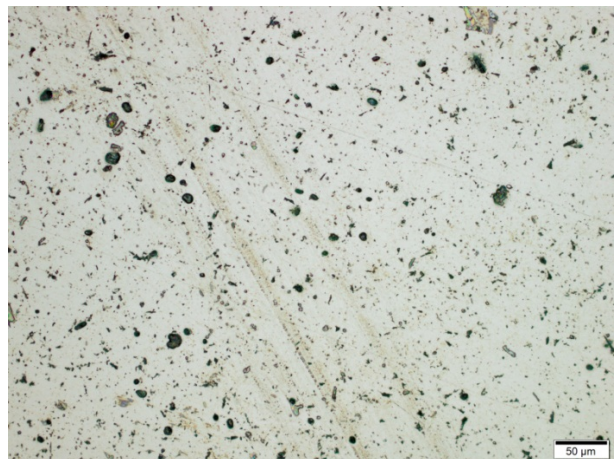


Figure 31(b). Wear scar of MoN-Cu flat

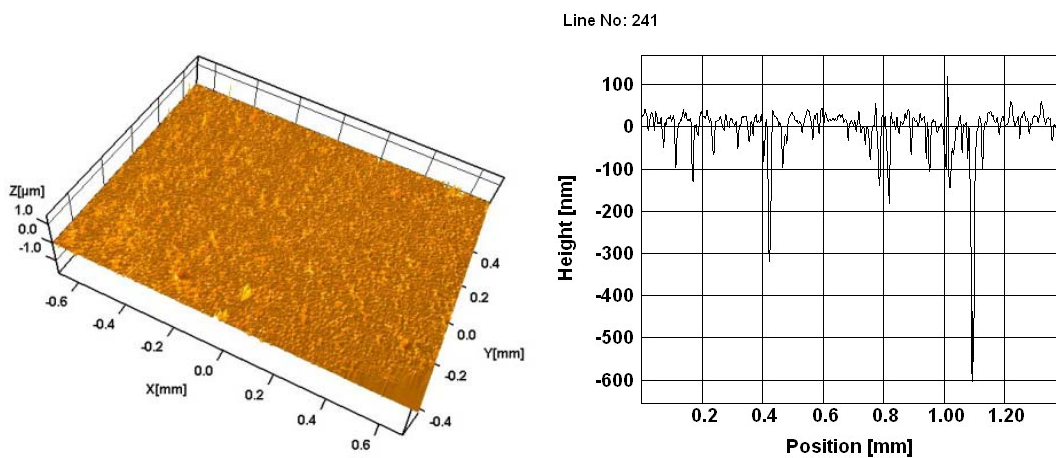


Figure 31(c). Wear scar profilometry of the flat with line scan

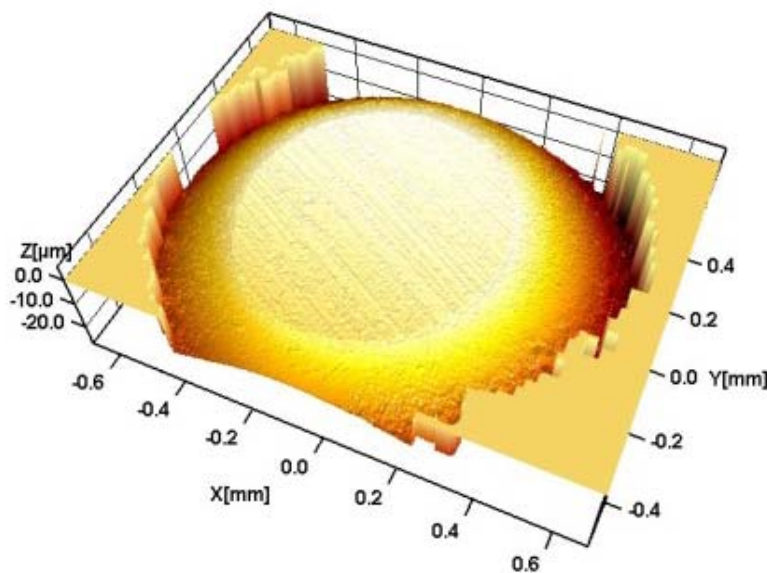


Figure 31(d). 3D-Wear scar profilometry of the ball

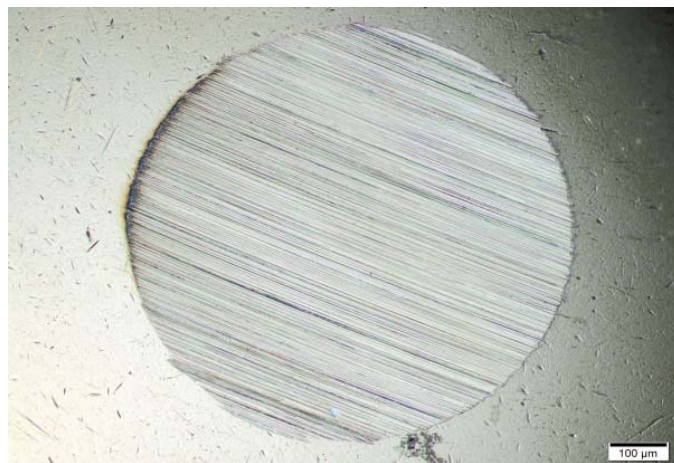


Figure 31(e). Ball micrograph

5) Tribological characterization of MoN-Cu flat vs 52100 steel ball with lubricant 5W30

Friction and wear of these coatings are studied with a ball on flat tribometer. Following are the conditions used in this test. A $\frac{1}{4}$ " 52100 steel ball was used for this test. The normal load was set to 2N with a track diameter of 30 mm and 10 rpm resulting in a linear speed of 16mm /s. The relative humidity of the surrounding is held at 44% and the total run lasted for 1800 sec. completing about 300 revolutions per run. This test involved Valvoline 5W30 as the lubricant. Figure 32(a) shows the friction trace from this test. The average coefficient of friction began with a higher value around 0.17 and reduced to 0.1 towards the end of the test. The wear on the flat could not be seen. Figure 32(b) show micrograph of the ball wear scar. It is evident from Figure 32(b) that the steel ball has reasonable wear at the contacting area.

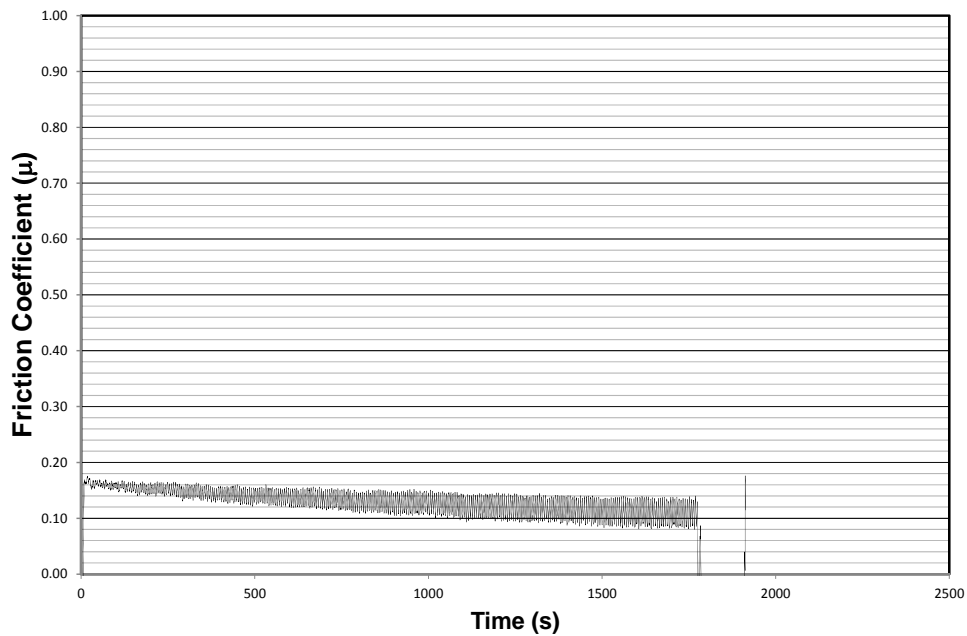


Figure 32(a). Friction trace, Friction coefficient Vs Time

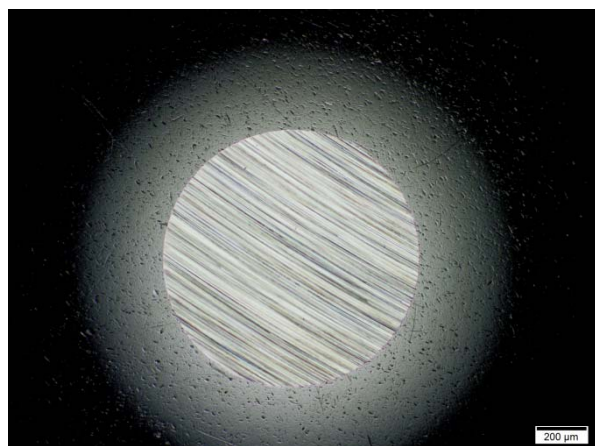


Figure 32(b). Ball micrograph (reasonable wear)

5.0 BENEFITS ASSESSMENT

Potential energy savings, related financial benefits and environmental protection

Our tool coatings are developed for applications in fabricated metal product section of manufacturing that consumed 388 trillion Btu in 2008. To approximate the machining sectors' energy saving potential, it was assumed that new coatings developed in this project would have gained a one-third of the market share by 2021 and these coatings would at least able to improve tool life by a modest 2X (over current average tool life). The U.S. annual energy saving would be close to 71.5 trillion Btu/year. With further optimization, we expect 6X improvement in tool life, hence energy saving figures will be much higher. Furthermore, with widespread utilization of high speed machining, the productivity will increase plus fewer machine down time and reject parts resulting from the uses of new coatings are expected to result in additional savings.

The coatings developed in die casting area can save energy in the metal casting industry that uses an estimated 200 to 250 trillion Btu. This includes energy from electricity, natural gas, propane and fuel oil. The energy used in metal casting is mostly in the melting, molding and heat treatment process, and consists of electric power and natural gas. Metal casting industry sales in the United States have been in the range of \$25 to \$28 billion annually for the past several years, with a small trade surplus. There are close to 3,000 foundries operating in all 50 states, employing one-quarter of a million people. The die-casting industry estimates show that 25% of the cost of the products (valued at nearly \$ 6.25 to 7 billion; (www.afsinc.org) is accounted for by the energy consumption. Thus, longer die life and longer production cycles will make a significant impact on the overall energy consumption rate (in terms of BTU/ton of product shipped), if developed coatings can be successfully implemented and commercialized. A 5% savings in energy would lower the energy consumption by 10 to 12.5 trillion Btu.

6.0 COMMERCIALIZATION

UES has successfully commercialized products and services in many of our core competencies. We successfully spun off three companies in the 1990's and early 2000's: 1) Paravant, Inc.- a portable command, control, 2) KI Shell™ - a workflow process management software 3) ProCAST™ - a software product providing simulations for casting and process design. These products generated over \$175,000,000 in cumulative commercial sales for UES. UES received the Tibbett's award in 2002, a prestigious award that exemplifies the very best in SBIR achievement and has an impressive Commercialization Achievement Index (CAI) of 100%, indicating the amount of commercialization efforts in comparison to SBIR awards,

As a commercialization effort for these novel high performing coatings, UES approached our present customers. UES is a Tier1 supplier to Honda of America for coated core pins. Honda has started using our new coatings in some of their applications. UES has recently established a Business Development group comprised of a senior manager, a direct sales engineer, and marketing and commercialization specialists. These personnel are assisted in the commercialization process by UES management and the Board of Directors. We have the appropriate technical and business teams in place to engineer the proposed technology, and bring it to market.

7.0 CONCLUSION

In this project, different aspects of the cutting tool and die casting tool degradation problems were investigated in detail. We realized the relevant issues that need to be addressed before an effective remedy can be proposed. Keeping requirements in focus, we have developed two novel coatings, Greycho ITM and Greycho IITM for cutting tools and highly potent Titan Generation IITM for die casting tools.

Greycho IITM was found to be very promising for deep roughening for hardened steel and received very good evaluation results from its commercial use. Hafnium diboride (HfB₂) based Titan Generation IITM also provided added protection to die casting pins as reported by Honda of America from their commercial use.

Argonne National Laboratory developed another material system based on MoN-Cu and successfully applied it on cutting tools and flats. These coatings have provided excellent wear data in both dry conditions and lubricated wearing conditions.

The anticipated energy and economic benefits resulted from these technologies can be substantial if it is fully developed, optimized and commercialized for various machining conditions and die casting applications

8.0 ACCOMPLISHMENTS

In this project, we have developed two novel coatings that could significantly improve tool life used for hardened steel deep roughening and improve the life of core pins used in aluminum die-casting. A low temperature CVD process was optimized to deposit the die casting coating.

In cutting tool life study, we have developed a new accelerated life test and came up with a novel tool life assessment technique based on optical microscopy of discoloration of used cutting tools of same geometry. This test could reasonably predict the out-come of our coating performance in commercial use.

Our most recent results from our tool coating study was presented at last year's Annual meeting of Society of Tribologists and lubrication Engineers (STLE) held on 8-12 of May 2011 in Atlanta GA. The title of the presentation was "Multiphase Nanostructure Coating for Cutting Tool Application". The authors of this presentation were Jose Nainaparampil, A.K. Rai and Rabi Bhattacharya from UES Inc.

9.0 **REFERENCES**

1. R. Buhl, H.K. Pulker, E. Moll, Thin Solid Films 80 (1981) 265.
2. G. Paller, B. Matthes, W. Herr, E. Broszeit, Mater. Sci. Eng., A 140 (1991) 647.
3. X.T. Zeng, S. Zhang, L.S. Tan, J. Vac. Sci. Technol., A 19 (2001) 1919.
4. S. Yang, D.G. Teer, Surface Engineering 18 (2002) 391–396.
5. Y.C. Chim , X.Z. Ding, X.T. Zeng , S. Zhang, Thin Solid Films 517 (2009) 4845–4849
6. A.J. Sue, A.J. Perry and J. Vetter, Scaf. Coat. TectmoI., 68/69 (1994) 126.
7. D.T. Quinto, 9". Vac. Sci. Teehnol., A,6 (1988) 2149.
8. O.A. Johansen, J .H. Dontje and R.L.D. Zenner, Thin Solid Films, I53 (1987) 75.
9. D.T. Quinto, G.J. Wolfe and P.C. Jindal, Thin Solid Films, 153 (1987) 19.
10. A.K.Rai, H.D.Lee, and Tai-il Mah, “Development of Ceramic Tool Material and Advanced Multifunctional Coatings for Improved Titanium Machining Process”, Phase I SBIR (contract # F33615-01-M-5301) Final Report, January 2002.
11. A. K. Rai and R. S. Bhattacharya “ Development of Hard-Soft Coatings for Enhanced Machining Performance Employing Large Area Filtered Arc deposition Technique”.The Edison Materials Technology Center, Dayton, OH 45420, Final Report, October 2006.
12. J. Vetter, W. Burgmer, H.G. Dederichs and A.J. Perry, Swf. Coat. Technol., 61 (1993) 209.
13. S.Y. Lee, S.D. Kim, Y.S. Hong, Surf. Coat. Technol. 193 (2005) 266.
14. T. Arai, Transactions of 18th NADACA International Die-Casting Congress, Paper No. T95-102 (1995).
15. J. Lin, S. Bhattacharya, S. Myers, B. Mishra, J.J. Moore, NADCA, 110 Metal Casting Congress Columbus Oh 2006
16. R.L. Boxman, P.J. Martin, D. Sanders, Eds., Handbook of Vacuum Arc Science and Technology, Noyes, New York, 1996.
17. <http://rsb.info.nih.gov/ij>